Optimization of the Pharmacophore Model for 5-HT$_7$R Antagonism. Design and Synthesis of New Naphtholactam and Naphthosultam Derivatives

María L. López-Rodríguez,*,† Esther Porras,† M. José Morcillo,‡ Bellinda Benhamú,† Luis J. Soto,† José L. Lavandera,† José A. Ramos,§ Mireia Olivella,|| Mercedes Campillo,|| and Leonardo Pardo||

Departamento de Química Orgánica I, Facultad de Ciencias Químicas, and Departamento de Bioquímica y Biología Molecular III, Facultad de Medicina, Universidad Complutense, E-28040 Madrid, Spain, Facultad de Ciencias, Universidad Nacional de Educación a Distancia, E-28040 Madrid, Spain, and Laboratori de Medicina Computacional, Unitat de Bioestadística and Institut de Neurociències, Universitat Autònoma de Barcelona, E-08193 Cerdanyola del Vallès, Barcelona, Spain

Received March 13, 2003

We present in this study an optimization of a preliminary pharmacophore model for 5-HT$_7$R antagonism, with the incorporation of recently reported ligands and using an efficient procedure with the CATALYST program. The model consists of five features: a positive ionizable atom (PI), a H-bonding acceptor group (HBA), and three hydrophobic regions (HYD). This model has been supported by the design, synthesis, and biological evaluation of new naphtholactam and naphthosultam derivatives of general structure **I** (**39**−**72**). A systematic structure−affinity relationship (SAFIR) study on these analogues has allowed us to confirm that the model incorporates the essential structural features for 5-HT$_7$R antagonism. In addition, computational simulation of the complex between compound **56** and a rhodopsin-based 3D model of the 5-HT$_7$R transmembrane domain has permitted us to define the molecular details of the ligand−receptor interaction and gives additional support to the proposed pharmacophore model for 5-HT$_7$R antagonism: (i) the HBA feature of the pharmacophore model binds Ser$^{5.42}$ and Thr$^{5.43}$, (ii) the HYD1 feature interacts with Phe$^{6.52}$, (iii) the PI feature forms an ionic interaction with Asp$^{3.32}$, and (iv) the HYD3 (AR) feature interacts with a set of aromatic residues (Phe$^{3.28}$, Tyr$^{7.43}$). These results provide the tools for the design and synthesis of new ligands with predetermined affinities and pharmacological properties.

Introduction

Serotonin (5-hydroxytryptamine, 5-HT) is an important neurotransmitter discovered over 50 years ago and, at present, it continues to generate interest as one of the most attractive targets for medicinal chemists. Molecular cloning and gene expression techniques have led to the characterization of 14 serotonin receptor subtypes, which can be classified in seven subfamilies (5-HT$_{1-7}$)[1−4] based on pharmacological properties, second messenger coupling, and sequence data. These receptors belong to the seven transmembrane G protein-coupled receptor superfamily (GPCRs),[5,6] except the 5-HT$_3$ receptor, which is a ligand-gated ion channel. 5-HT$_7$ is the most recent addition to the burgeoning family of 5-HT receptors that was identified from cloning studies before the corresponding endogenous receptor was found.[7,8] This receptor is positively coupled to adenylyl cyclase through G_s when expressed in cell lines.[9] The 5-HT$_7$ receptor (5-HT$_7$R) has been cloned from mouse,[10] rat,[11,12] guinea pig,[13] and human[14] and exhibits a low sequence homology with other 5-HT receptors. The binding profile appears consistent across species and between cloned and native 5-HT$_7$Rs. Splice variants have been identified[15−17] in rat and human that display similar tissue distribution and pharmacological and functional characteristics. Although the biological functions of the 5-HT$_7$R have not been fully clarified, early pharmacological data suggest that this subtype may be involved in disturbance of circadian rhythms,[18,19] such as jet lag and delayed sleep-phase syndrome. Therefore, a 5-HT$_7$R antagonist might be a useful therapeutic agent for the treatment of sleep disorders. It is also believed that a deregulated circadian rhythm could lead to mental fatigue and depression. Thus, one of the consequent mechanisms of antidepressant treatment could be the modulation of a possible dysrhythmic circadian function in depression, in which the 5-HT$_7$R might be one of the key players.[20] The fact that antipsychotic agents exhibit a high affinity for the 5-HT$_7$R leads to the speculation that this receptor might provide a target for the treatment of psychotic disorders.[21−24] In the periphery, the 5-HT$_7$R plays a role in smooth muscle relaxation in a variety of tissues[25−30] and so it might be involved in diseases such as irritable bowel syndrome[31] or migraine.[32] Nevertheless, the therapeutic utility of 5-HT$_7$R agents awaits the development of selective ligands. Despite intense research efforts in this area, very few compounds with significant 5-HT$_7$R antagonist activity have been reported and, to date, only five selective antagonists belonging to two structural classes of compounds (SB-258719,[33] DR4004,[34] SB-269970,[35] DR4365,[36] and DR4485[37]) have been discovered by high-throughput screening. Information on the structural properties of the 5-HT$_7$R agents remains unknown and its determi-

* To whom correspondence should be addressed. Phone: 34-91-3944239. Fax: 34-91-3944103. E-mail: mluzlr@quim.ucm.es.
† Departamento de Química Orgánica I, Facultad de Ciencias Químicas, Universidad Complutense.
‡ Universidad Nacional de Educación a Distancia.
§ Departamento de Bioquímica y Biología Molecular III, Facultad de Medicina, Universidad Complutense.
|| Universitat Autònoma de Barcelona.

10.1021/jm030841r CCC: $25.00
Published on Web 11/08/2003

nation represents a critical step for developing specific compounds.

In this context it is important to derive putative 3D pharmacophore models, and we have recently postulated a pharmacophore model for 5-HT_7R antagonism,[38] as an initial step in the course of an extensive program targeted at the discovery of new serotonin 5-HT_7R ligands.

In the present work, with the aim of gaining insight into the pharmacophoric patterns responsible for 5-HT_7R affinity, we have carried out an optimization of this preliminary hypothesis with the incorporation of recently reported antagonists and using a systematic and efficient procedure with the CATALYST program.[39] Subsequently, the identified 3D pharmacophore was used to search flexible 3D databases to discover novel chemical entities that could provide knowledge for the design of new lead compounds. On the basis of these results and in order to give support to our model, new designed analogues of general structure **I** (**39**−**72**) were synthesized and evaluated for affinity at the 5-HT_7R. The analysis of the influence of some structural variations of the different pharmacophoric elements on the affinity for the 5-HT_7R of this class of compounds led us to confirm the essential requirements postulated for 5-HT_7R antagonism. Moreover, computational simulations of the complex between compound **56** and a 3D model of the transmembrane domain of the receptor have permitted the identification of the molecular determinants of recognition of these ligands by the 5-HT_7R.

Computational Methods

Pharmacophore Model for 5-HT_7R Antagonists. Compounds **1**−**38** were built de novo using standard options within the 2D/3D editor sketcher of the CATALYST 4.5[39] program. In cases where the chirality of the active form is not known, all possible stereoisomers were generated and considered. Each compound is treated as a collection of conformers covering the accessible conformational space within an energy range.[40,41] The BEST conformational analysis procedure was applied. The number of conformers was limited to a maximum of 250 and with 25 kcal/mol energy threshold above the calculated global minimum as estimated with the CHARMm-like force field.[40,42,43]

CATALYST 4.5[39] software supports the HypoGen algorithm, which is able to generate pharmacophoric hypotheses from a set of compounds known to be active at a specific target, by means of identification of common features present in the active but absent in the inactive molecules of the training set. Previously reported models developed by HypoGen have been successfully used to suggest new directions in lead discovery[44−49] and for searching databases to identify new structural classes of potential lead candidates.[50] The following values were chosen: spacing (1.00−2.95 Å), weight variation (1.0), tolerance variation (1.0), mapping coefficient (0), and activity uncertainty (3). Hypothesis selection is done by a cost analysis procedure. The cost function consists on three terms: the weight cost, which increases in a Gaussian form as the feature weight in a model deviates from an idealized value of 2.0; the error cost, which penalizes the deviation between the estimated activities of the training set and their experimentally determined values; and the configuration cost, which penalizes the complexity of the hypothesis. Of these three, the error cost contributes the most in determining the overall cost of a hypothesis. The 10 lowest energy cost hypotheses are extracted and analyzed. Moreover, the cost of two theoretical hypotheses [the ideal hypothesis, which is the simplest possible hypothesis that fits the data with minimal cost (fixed cost), and the null hypothesis, where the error cost is high (null cost)] are computed. These fixed and null cost values represent the minimum and maximum energy cost values, respectively. The greater their difference, the higher the probability of finding predictive models (>60 bits, >90%; 40−60 bits, 75−90%; <40 bits, <75%).

3D-Database Searching. A database search has been performed using the "best flexible search" method provided by CATALYST 4.5.[39] The defined pharmacophore model was built into a 3D query, which included pharmacophoric features (HBA, PI, HYD1, HYD2, and HYD3) and distance ranges between the crucial components of the pharmacophore. The conformational models stored in the databases are allowed to flex in order to map the 3D query. The NCI (National Cancer Institute), Maybridge, MiniBioByte, and Sample databases (provided with CATALYST 4.5), containing a total of approximately 178 600 compounds, were searched.

Model of the Complex between Compound 56 and the 5-HT_7R. The construction of the 3D model of the transmembrane domain of the 5-HT_7R was performed in a manner similar to the recently described model of the 5-HT_4R.[51] This computer model maintains the position of the transmembrane helices (TMHs) as in rhodopsin[52] with the exception of TMH 3. TMH 3 is slightly bent toward TMH 5, at position 3.37 (receptor-numbering scheme of Ballesteros and Weinstein[53]), to facilitate the experimentally derived interactions between the ligand and the conserved $Asp^{3.32}$, in TMH 3, and a series of conserved Ser/Thr residues (5.42 and 5.43), in TMH 5. This structural effect is due to the gauche-conformation of the $Thr^{3.37}$ side chain.[54] We have recently provided experimental evidence for this structural difference of TMH 3 in rhodopsin and the serotonin family by designing and testing ligands that contain comparable functional groups but at different interatomic distances.[55]

The mode of recognition of the naphtholactam moiety of the ligand was first determined by ab initio geometry optimization with the ONIOM procedure.[56] The model system consisted of $Val^{3.33}$, $Ile^{4.56}$, $Ser^{5.42}$, $Thr^{5.43}$, and $Phe^{6.52}$ (only the C_α atom of the backbone is included) of the 5-HT_7R and the ligand **56** [the $-(CH_2)_5-$ chain plus the piperazine and phenyl rings were replaced by a methyl group]. All free valences were capped with hydrogen atoms. The C_α atoms of the residues were kept fixed at the positions obtained in the 5-HT_7R model. The ONIOM procedure allows the molecular system to be divided into three layers that are treated at different levels of theory: ligand **56** and $Phe^{6.52}$ at the MP2/6-31G* level of theory, which is capable of describing the proposed C−H$\cdots\pi$ interactions;[57] $Ser^{5.42}$ and $Thr^{5.43}$ at the B3LYP/6-31G level of theory; and $Val^{3.33}$ and $Ile^{4.56}$ at the semiempirical AM-1 level of theory.

This optimized reduced model of the ligand−receptor complex was used to position compound **56** inside the

Table 1. Training Set Used in the Generation of the Pharmacophore for Selective 5-HT$_7$R Antagonists

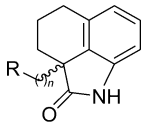

no.	*n*	R	pK_i expl.[a]	pK_i est.
1	2	4-phenylpiperazin-1-yl	7.0	7.7
2	3	4-phenylpiperazin-1-yl	8.3	7.4
3	4	4-phenylpiperazin-1-yl	8.5	8.0
4	4	4-(2-methoxyphenyl)piperazin-1-yl	8.3	8.4
5	4	4-(2-cyanophenyl)piperazin-1-yl	8.4	8.1
6	4	4-(2-pyridyl)piperazin-1-yl	8.7	8.4
7 (DR4004)	4	4-phenyl-1,2,3,6-tetrahydropyridyl	8.7	8.7
8	4	4-cyclohexylpiperazin-1-yl	4	5.2

[a] Values reported in ref 34.

entire transmembrane domain of the 5-HT$_7$R. Subsequently, the ligand−receptor complex was placed in a rectangular box (∼76 Å × 77 Å × 64 Å in size) containing methane molecules (7312 molecules in addition to the transmembrane domain) to mimic the hydrophobic environment of the transmembrane helices. It has been shown that this procedure reproduces several structural characteristics of membrane-embedded proteins.[58] Finally, the complete system was energy-minimized using the particle mesh Ewald method to evaluate electrostatic interactions and a 13 Å cutoff for nonbonded interactions. Parameters for the system were obtained from the Cornell et al. force field[59] and the "general Amber force field" using RESP point charges.[60]

Quantum mechanical calculations were performed with the GAUSSIAN-98 system of programs.[61] Energy minimizations were run with the Sander module of AMBER7.[62]

Results and Discussion

Conformational Analysis with Catalyst. A total of 38 reported compounds were selected[10−12,14,33−35,63−65] as a training set in the generation of a pharmacophoric model for 5-HT$_7$R antagonists. Their 2D chemical structure and binding affinities are represented in Tables 1−5 and Chart 1. The structural diversity and wide range of affinities, spanning 5 orders of magnitude, from 1.3 nM to 100 μM, are necessary to obtain meaningful results. A conformational analysis was performed, as described in the Computational Methods section, for the compounds in the training set. In our case, an almost balanced distribution of axial and equatorial substituents on the piperazine ring (representing the most favorable conformations) was highlighted. In addition, twisted or even orthogonal conformations of the piperazine with respect to the phenyl ring of the arylpiperazine moiety of the ligands were also found. These results were compared with Molecular Dynamics and Monte Carlo conformational searches carried out on these piperazine derivatives.

The library of the chemical descriptors in the program[66] was used to map the chemical functionalities of each molecule. The following kinds of surface-accessible functions were considered for pharmacophore generation: hydrogen bond acceptor (HBA), hydrophobic group (HYD), positively ionizable center (PI), and aromatic ring (AR). The obtained conformations of each compound were used to align these chemically important functional groups, and pharmacophoric models were then generated from the aligned structures.

As an initial approach, a training set of 38 compounds from different chemical series, described in the literature as selective and nonselective 5-HT$_7$R antagonists, were used to generate pharmacophore models with CATALYST. The best hypothesis obtained (hypothesis 1 in Table 6), with one hydrogen-bond acceptor (HBA), two hydrophobic (HYD) features, one positive ionizable (PI) group, and one aromatic ring (AR) feature, presented a low correlation coefficient (0.7396). Thus, to improve this poor statistic, we removed the nonselective compounds (**25**−**38**) from the training set, with the aim of identifying a statistically significant 3D arrangement of chemical functions that explains the selective affinity for the 5-HT$_7$R. It is important to note that attempts to obtain a pharmacophore model using the nonselective set (**25**−**38**) leads to models with a low predictive power (the difference between null and fixed cost is lower than 35; results not shown).

Pharmacophore Model for Selective 5-HT$_7$R Antagonists. Sets of 10 hypotheses were generated with compounds **1**−**24**. Table 6 shows the best hypotheses obtained, listed as 2−6, with different cost values, correlation coefficients, and pharmacophore features. Hypotheses 2 and 3 have five chemical features in a similar spatial location, their only difference being the replacement of one of the hydrophobic features found

Table 2. Training Set Used in the Generation of the Pharmacophore for Selective 5-HT$_7$R Antagonists

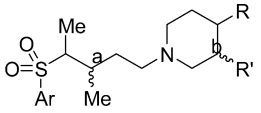

no.	Ar	R	R	stereochemistry a	stereochemistry b	pK_i expl[a]	pK_i est.
9	1-naphthyl	H	Me	*R*	*R*	6.9	6.8
10	1-naphthyl	H	Me	*R*	*S*	6.2	6.5
11	1-naphthyl	H	Me	*S*	*R*	5.8	6.1
12	1-naphthyl	H	Me	*S*	*S*	4	6.0
13 (SB-258719)	3-methylphenyl	Me	H	*R*		7.5	7.7
14	1-naphthyl	Me	H	*R*		7.5	6.6
15	3,4-dichlorophenyl	Me	H	*R*		7.5	7.4
16	3,4-dibromophenyl	Me	H	*R*		7.7	7.7
17	4,5-dibromo-2-thienyl	Me	H	*R*		7.8	7.2

[a] Values reported in ref 33.

Table 3. Training Set Used in the Generation of the Pharmacophore for Selective 5-HT$_7$R Antagonists

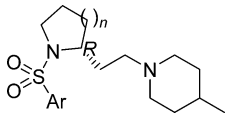

no.	Ar	*n*	pK_i expl[a]	pK_i est.
18	1-naphthyl	2	7.8	7.5
19	1-naphthyl	1	8.0	7.7
20	3,4-dichlorophenyl	1	8.4	8.7
21	3-bromophenyl	1	8.7	8.2
22 (SB-258741)	3-methylphenyl	1	8.5	8.0
23	3-methoxyphenyl	1	8.0	8.3
24 (SB-269970)	3-hydroxyphenyl	1	8.9	8.6

[a] Values reported in ref 35.

Table 4. Training Set Used in the Generation of the Pharmacophore for Nonselective 5-HT$_7$R Antagonists

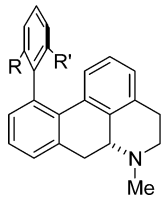

no.	R	R	pK_i(5-HT$_7$)[a]
25	OMe	OMe	7.9
26	CN	Me	8.4
27	OH	Me	7.6

[a] Values reported in ref 63.

Table 5. Training Set Used in the Generation of the Pharmacophore for Nonselective 5-HT$_7$R Antagonists

no.	compd	pK_i(5-HT$_7$)	refs
28	metergoline	8.2	12, 14, 64
29	mesulergine	8.1	12
30	2-Br-LSD	8.0	10
31	methylsergide	7.9	12
32	clozapine	7.9	12
33	(*S*)-methiothepine	9.0	12
34	cyproheptadine	7.3	12
35	mianserin	7.2	11
36	(+)-butaclamol	7.2[a]	10, 11
37	ritanserin	7.8	12
38	spiperone	7.7	11, 65

[a] This value represents the mean of different pK_i values reported in refs 10 and 11.

in hypothesis 2 with a more specific aromatic ring in hypothesis 3 (Figure 1a,b). On the basis of the very similar composition of the two hypotheses, hypothesis 2, characterized by the best statistical parameters (Table 6), has been chosen to represent the best candidate as a pharmacophore for 5-HT$_7$R selective compounds, which consist of a basic nitrogen atom (PI), a H-bonding acceptor group (HBA), and three hydrophobic regions (HYD) at the distances represented in Figure 1a. The HYD (blue) and PI (red) features are drawn as globes, whereas HBA (green) and AR (orange) features are shown as two globes due to the directional nature of these chemical functions.

The total cost of hypothesis 2 was 154.15. With a cost difference between fixed and null hypotheses of 48.95 bits, the probability that a true correlation exists in the data is high. On this hypothesis, all the compounds mapped the PI feature and at least one of the three HYD

Chart 1. 2D Chemical Structures of the Molecules of the Nonselective Training Set (**28**−**38**)

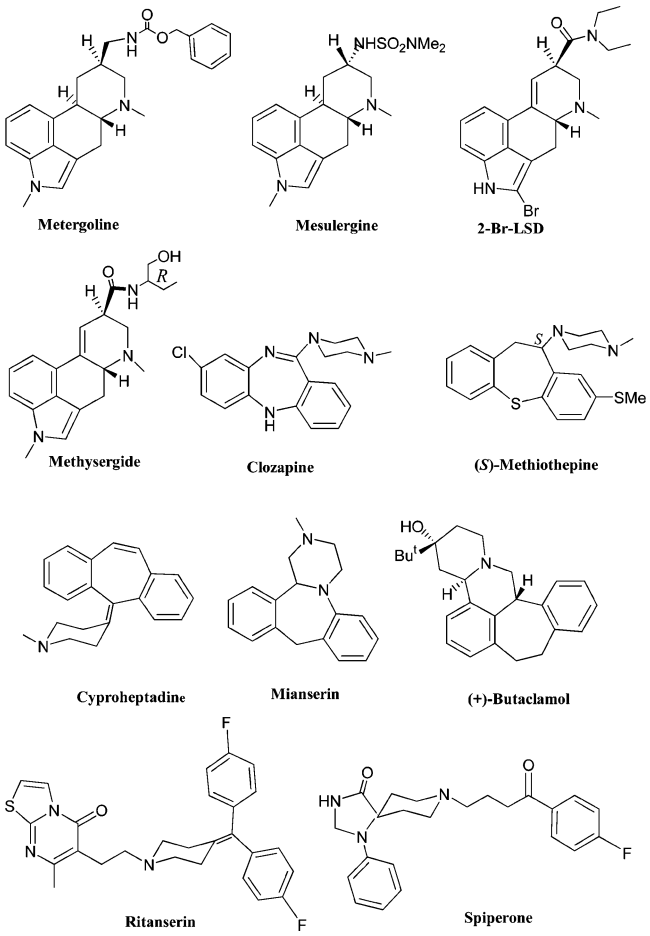

features, while the HBA was fitted by 62.5% of compounds. In Figure 2, the good predictive power of this model is indicated by the high correlation coefficient between experimental and estimated affinity values (r = 0.9123). As shown in Tables 1−3, for all the molecules in the training set this model is able to predict the affinity of compounds with reasonable precision. In this case a predicted pK_i value within 1 log unit of the experimental pK_i value was considered to be a valid prediction of fit. From these data in Tables 1−3 we can see that out of 10 highly active compounds (pK_i > 8), nine were accurately predicted as highly active and only one (compound **2**) was predicted as moderately active. Out of nine moderately active compounds (8 ≤ pK_i ≤ 7), one compound (**23**) was predicted as highly active and another one (**14**) was predicted as poorly active (pK_i < 7). Those compounds with low 5-HT$_7$R affinity (pK_i < 7) were correctly predicted.

Figure 1c,d shows DR4004 (**7**) and SB-269970 (**24**), the most active and selective compounds in the training set, placed into the pharmacophore model for selective 5-HT$_7$R antagonists. In detail, SB-269970 (**24**) fulfills HYD features through aliphatic regions, the HBA with the sulfonamide group, and the PI feature through the protonated nitrogen of the piperidine ring.

3D-Database Searching and Design. We have selected hypothesis 2 for selective 5-HT$_7$R antagonists as a better pharmacophore model (Figure 1a) to design and synthesize new 5-HT$_7$R ligands as a *test set* in order to evaluate the predictive power of the model. This

Table 6. Summary of All the Most Important Generated Hypotheses

hypothesis	training set[a]	features in the hypothesis[b]	cost			compd mappings
			fixed	total (correl)	null	
1	A = 38 compds	HBA, 2xHYD, PI, AR	166.906	215.294 (0.7396)	227.741	11 HBA; 14 HYD1; 29 HYD2; 36 PI; 38 AR
2	B = 24 selective compds	HBA, 3xHYD, PI	122.888	154.15 (0.9123)	171.836	15 HBA; 24 HYD1; 14 HYD2; 24 HYD3; 24 PI
3	B = 24 selective compds	HBA, 2xHYD, PI, AR	122.888	162.003 (0.8617)	171.836	19HBA; 23 HYD1; 24 HYD2; 24 PI; 6 AR
4	B = 24 selective compds	HBA, 2xHYD, PI, AR	122.888	164.424 (0.8857)	171.836	18HBA; 24 HYD1; 23 HYD2; 23 PI; 7 AR
5	B = 24 selective compds	HBA, 3xHYD, PI	123.158	154.788 (0.9043)	171.836	15 HBA; 24 HYD1; 13 HYD2; 23 HYD3; 24 PI
6	B = 24 selective compds	HBA, 2xHYD, PI, AR	123.158	162.537 (0.8539)	171.836	16 HBA; 24 HYD1; 24 HYD2; 24 PI; 7 AR

[a] 38 compds = whole set of compounds selective + nonselective. [b] HBA, hydrogen bond acceptor; HYD, hydrophobic; PI, positive ionizable; AR, aromatic ring.

pharmacophore model was used as a 3D query to perform a database search to find other structural motifs that fulfill the functional and spatial constraints imposed by the model itself. Several databases (see Computational Methods), containing approximately 178 600 compounds, were searched.

On the basis of the analysis of these results, a new series of derivatives of general structure **I** with synthetic accessibility were designed as *test set* (Figure 3a). Conformational analysis reveals that compounds with an optimum length of four or five methylene units for the spacer map fit in an efficient way the hypothesis 2. For example, in compound **51** (X = CO, n = 4, Y = N, R = phenyl) an aromatic ring of the naphtholactam system fits within HYD1, the carbonyl group acts as HBA, the basic nitrogen atom fits within the PI, the piperazine ring fits within HYD2, and the phenyl ring is HYD3 (Figure 3b). Thus, we have considered the synthesis, biological evaluation, and initial SAR investigations of compounds **39**−**72** (Table 7) with the aim of giving support to the proposed pharmacophore model and confirming the optimum spacer length.

Chemistry. The synthetic routes used in the preparation of **39**−**72** are outlined in Scheme 1. Compounds **39** and **40** (n = 1) were obtained by Mannich reaction of benzo[*cd*]indol-2(1*H*)-one (naphtholactam) with formaldehyde and the appropriate arylpiperazines (method A). Treatment of 1-aryl-4-(3-chloropropyl)piperazines **73** and **74** with naphtholactam, in the presence of sodium hydride and *N*,*N*-dimethylformamide (DMF), gave **41** and **42** (method B). Desired compounds **43**−**71** (n = 4−6) were obtained by reaction of intermediates **75**−**80** with the appropriate amines in the presence of triethylamine in acetonitrile as solvent (method C). Preparation of compound **72** was performed by reaction of **75** with 1-methyl-1*H*-imidazole-2-thiol in the presence of sodium methoxide and methanol as solvent (method D). Treatment of 1-arylpiperazines with 1-bromo-3-chloropropane, in the presence of potassium carbonate and DMF, gave the corresponding intermediates **73** and **74**. The key derivatives **75**−**80** were prepared by reaction of naphtholactam or naphthosultam with the appropriate dibromoalkane in the presence of sodium hydride and DMF. Amines **81**−**83** were obtained by catalytic hydrogenation of corresponding pyridines. Respective hydrochloride salts were prepared as samples for biological assays. All new compounds were characterized by IR and ^{1}H and ^{13}C NMR spectroscopy and gave satisfactory combustion analyses (C, H, N).

Biochemistry. The 5-HT$_7$R binding affinity of synthesized compounds **39**−**72** was determined by measurement of the displacement of [^{3}H]-5-CT binding in rat hypothalamus membranes.[68] All the compounds were used in form of hydrochloride salts and were methanol-soluble. The inhibition constant K_i was calculated from the IC_{50} by the Cheng−Prusoff equation.[69] The results of these assays are illustrated in Table 7. Additionally, compound **56** was evaluated in a previously described functional model of 5-HT$_7$ receptor activation,[70] blocking 5-carboxamidotryptamine (5-CT)-stimulated adenylyl cyclase activity, indicating its antagonist profile.

Structure−**Affinity Relationship Studies.** One of the most important facts observed in the analysis of the results presented in Table 7 is that all the synthesized compounds that possess a significant affinity for the 5-HT$_7$R share all the chemical features of our pharmacophore model [e.g., pK_i(**52**) = 7.2, pK_i(**56**) = 7.1, and

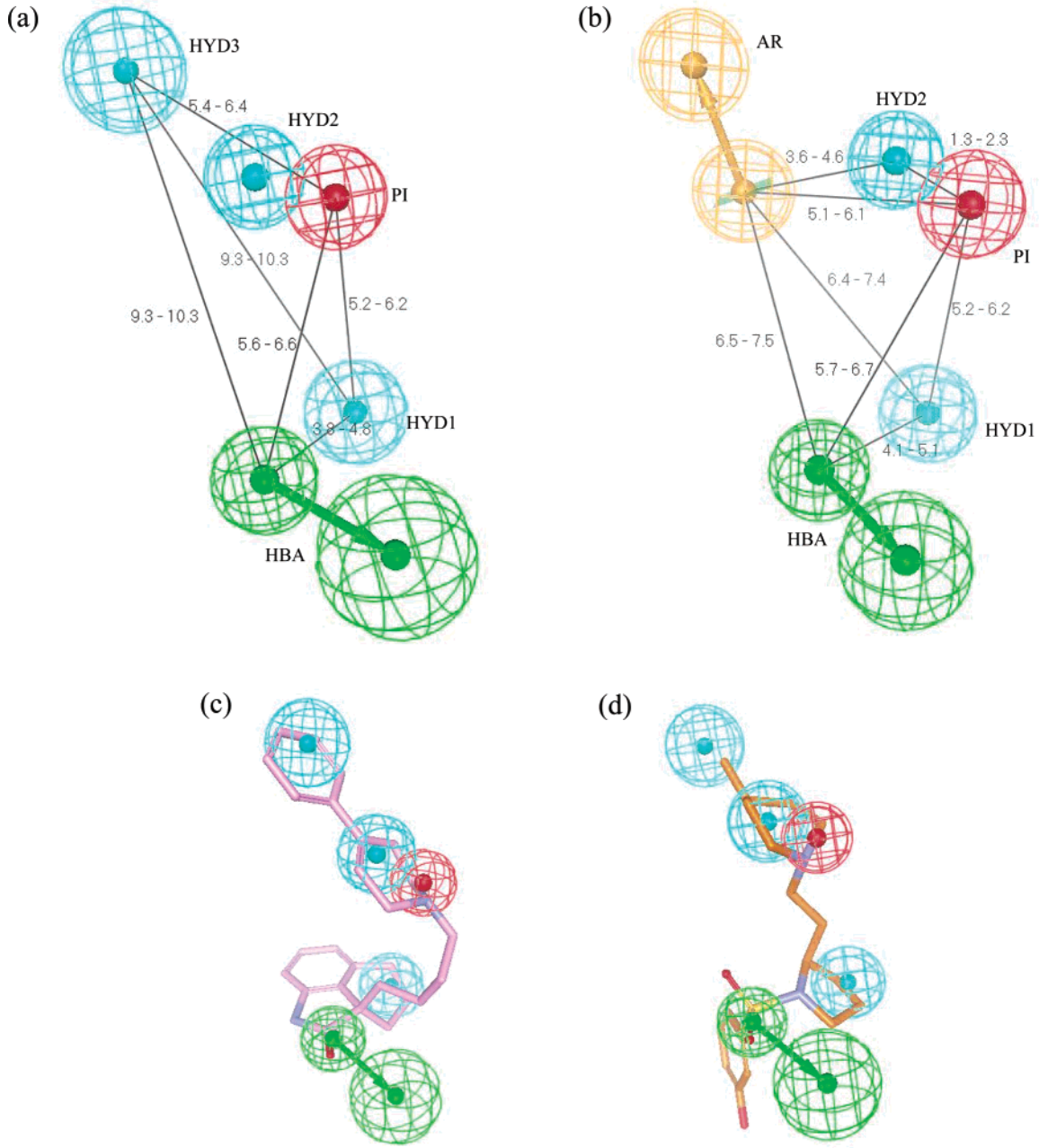

Figure 1. Pharmacophore models for selective 5-HT$_7$R antagonists: (a) hypothesis 2 and (b) hypothesis 3. Most active compounds in the selective training set, mapped onto hypothesis 2: (c) DR4004 (**7**) and (d) SB-269970 (**24**).

pK_i(**57**) = 7.0]. In contrast, derivatives that lack any of the pharmacophoric features required for 5-HT$_7$R antagonism are inactive; for instance, inactive compounds **39**−**42** lack the appropriate distance of 5.6−6.6 Å between HBA and PI. In this series the hydrophobic region (HYD3) situated at a distance of 5.4−6.4 Å from the nitrogen atom (PI) should be a more specific aromatic ring. Thus compounds with a nonaromatic moiety fitting within HYD3 are inactive [e.g. compounds **49** and **62** (R = methyl) and **50** and **55** (R = cyclohexyl)].

Study of the relationship between the structure and affinity of this class of compounds has given support to the pharmacophoric requirements postulated and has led to the following conclusions: (i) It can be observed that the optimum spacer length is four or five methylene units, since compounds with $n = 1$ or 3 are inactive [e.g. analogues **39** ($n = 1$) and **41** ($n = 3$): pK_i < 5]. An exception is represented by derivative **42** with a 3-carbon chain in the spacer (pK_i(**42**) = 6.4), but this compound has less affinity than **52** ($n = 4$, pK_i(**52**) = 7.2). An increase in the size of the alkyl chain to $n = 6$ causes a retention or moderate decrease in the binding affinity [e.g., pK_i(**64**) = 6.7 vs pK_i(**71**) = 6.7]. These results are in agreement with our pharmacophore model, which defines the optimum distance between the HBA and the basic center as 5.6−6.6 Å. Analogues with a shorter spacer than 5.6 Å ($n = 1$, 3) are inactive. The length of the spacer of derivatives bearing a 6-carbon chain may allow them to adopt a folded conformation with the appropriate distance to interact with the receptor. (ii) On the other hand, an examination of the binding data shows that naphtholactam derivatives are more potent at 5-HT$_7$R sites than naphthosultam analogues [e.g., pK_i(**52**) = 7.2 vs pK_i(**64**) = 6.7; pK_i(**57**) =

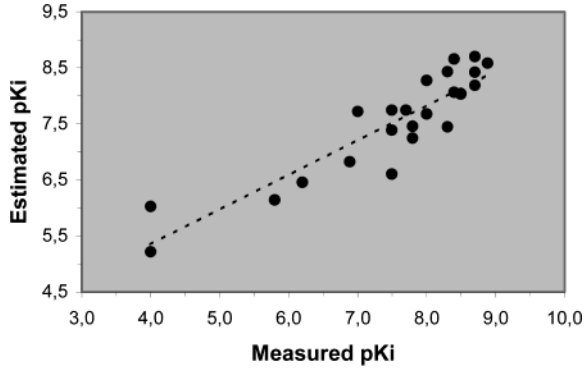

Figure 2. Correlation line displaying the experimental vs estimated affinity values by using the statistical most significant hypothesis of the selective training set (hypothesis 2), $r = 0.9123$.

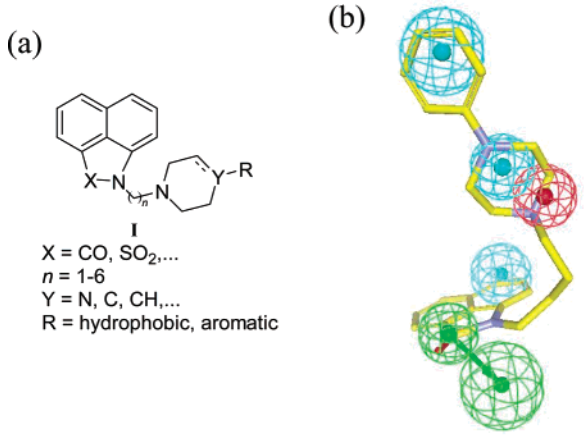

Figure 3. (a) Designed compounds of general structure **I**. (b) Compound **51** mapped on the pharmacophore model generated for selective 5-HT$_7$R antagonists (hypothesis 2).

7.0 vs pK_i(**68**) = 6.6)]. (iii) In general, replacement of the piperazine with a piperidine or tetrahydropyridine ring causes a dramatic loss in affinity. Thus, compound **51** (Y = N) shows 5-HT$_7$R affinity (pK_i = 6.2), while analogues **47** (Y = CH) and **48** (Y = C) are inactive (pK_i < 6). These findings clearly suggest that the nitrogen in position 4 of the piperazine ring plays an important role on 5-HT$_7$R affinity, in this kind of ligand. (iv) Our data indicate that the hydrophobic region HYD3 must be aromatic, since only compounds of general structure **I** with this *hydrophobic−aromatic* region show affinity for the 5-HT$_7$R. Thus, substitution of the phenyl moiety by a methyl or cyclohexyl group, as in compounds **51** vs **49** and **50**, led to a loss of affinity at the 5-HT$_7$R [pK_i(**51**) = 6.2 vs pK_i(**49**) < 5 and pK_i(**50**) < 5]. The only exception to this trend is analogue **45** (R = isopropyl), which is moderately active at the 5-HT$_7$R [pK_i(**45**) = 6.7]. (v) The isosteric change of basic piperazine moiety for an imidazole seems to have a negative influence on the 5-HT$_7$R affinity [e.g. pK_i(**56**) = 7.1 vs pK_i(**72**) < 5). These data might suggest that the interaction between the protonated nitrogen of the piperazine and the receptor is electrostatic, and it is not due to prototropic equilibrium.

These findings have allowed us to conclude that the resulting model provides significant correlation between the chemical structures of the synthesized compounds and their biological data, and confirms that the proposed pharmacophore model for 5-HT$_7$R antagonism incorporates the essential structural features. Further synthesis and biological evaluation of new derivatives are currently in progress.

Table 7. Binding Affinity of Synthesized Compounds at 5-HT$_7$Rs

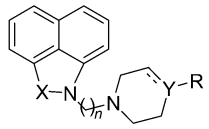

I

Comp.	X	*n*	Y	R	pK_i±SEM[a]
39	CO	1	N	phenyl	<5
40	CO	1	N	*o*-methoxyphenyl	<5
41	CO	3	N	phenyl	<5
42	CO	3	N	*o*-methoxyphenyl	6.4±0.06
43	CO	4	CH	H	<5
44	CO	4	CH	methyl	<6
45	CO	4	CH	isopropyl	6.7±0.05
46	CO	4	CH	cyclohexyl	<6
47	CO	4	CH	phenyl	<6
48	CO	4	C	phenyl	<6
49	CO	4	N	methyl	<5
50	CO	4	N	cyclohexyl	<5
51	CO	4	N	phenyl	6.2±0.003
52	CO	4	N	*o*-methoxyphenyl	7.2±0.005
53	CO	5	CH	isopropyl	<6
54	CO	5	C	phenyl	<6
55	CO	5	N	cyclohexyl	<5
56	CO	5	N	phenyl	7.1±0.02
57	CO	5	N	*o*-methoxyphenyl	7.0±0.05
58	CO	6	N	phenyl	<6
59	CO	6	N	*o*-methoxyphenyl	<6
60	SO_2	4	CH	H	<5
61	SO_2	4	CH	methyl	<5
62	SO_2	4	N	methyl	<5
63	SO_2	4	N	phenyl	6.0±0.06
64	SO_2	4	N	*o*-methoxyphenyl	6.7±0.004
65	SO_2	5	CH	methyl	<5
66	SO_2	5	CH	cyclohexyl	<5
67	SO_2	5	N	phenyl	6.7±0.06
68	SO_2	5	N	*o*-methoxyphenyl	6.6±0.02
69	SO_2	6	CH	methyl	<5
70	SO_2	6	N	phenyl	<6
71	SO_2	6	N	*o*-methoxyphenyl	6.7±0.03
72	CO	4			<5
			DR4004		7.3[b]
			SB-256719		7.1[b]
			SB-269970		7.5[b]

[a] pK_i = −log K_i. K_i (M) values are means of two to four assays, performed in triplicate. Inhibition curves were analyzed by a computer-assisted-curve-fitting program (Prism GraphPad). [b] Data from ref 67 (in rat hypothalamus).

Model of the Complex between Compound 56 and the 5-HT$_7$R. Mutagenesis experiments on several GPCRs that bind biogenic amines have identified a series of conserved Ser/Thr residues (5.42 and 5.43), in TMH 5, which act as hydrogen-bonding sites for the hydroxyl groups present in the chemical structure of many neurotransmitters.[71,72] Thus, it seems reasonable to assume that the carbonyl group (X = CO) of the naphtholactam moiety of compound **56** interacts with the side chain of these Ser/Thr residues. Figure 4a shows the energy-minimized structure of the complex between this naphtholactam moiety and the side chains of Val$^{3.33}$, Ile$^{4.56}$, Ser$^{5.42}$, Thr$^{5.43}$, and Phe$^{6.52}$ that are forming its binding site in the 3D model of the transmembrane domain of the 5-HT$_7$R (see Computational

Scheme 1[a]

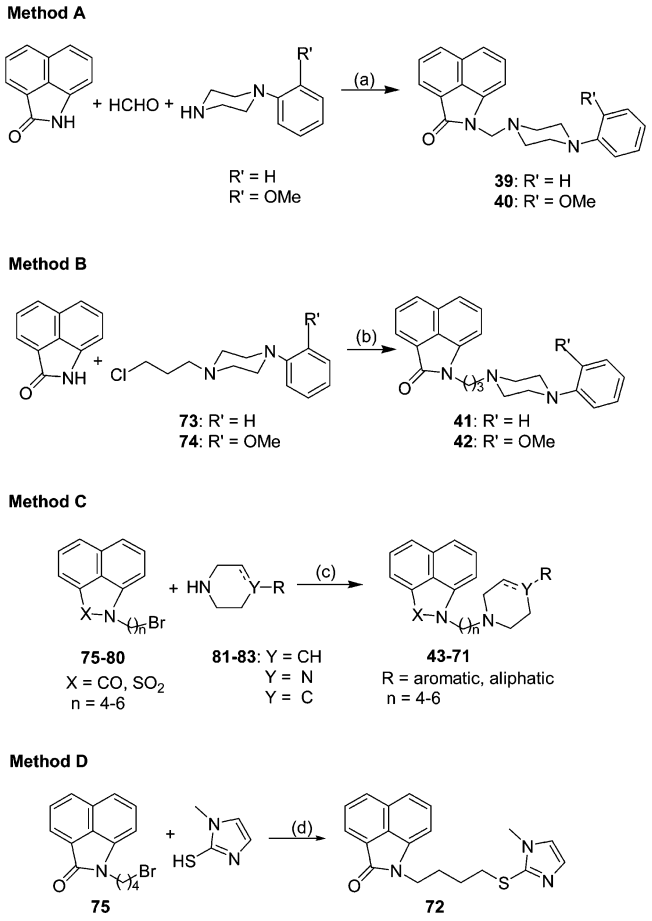

[a] Reagents: (a) EtOH; (b) NaH, DMF anh.; (c) Et_3N, CH_3CN; (d) MeONa, MeOH.

Methods for details). The carbonylic oxygen of the ligand is interacting with the hydroxyl groups of Ser$^{5.42}$ and Thr$^{5.43}$. It is important to note that the interaction of the ligand with these Ser/Thr residues would benefit from a less bulky aromatic ring. However, this extensive naphtholactam ring favors the $\pi-\sigma$ aromatic−aromatic interaction with the side chain of Phe$^{6.52}$ in the face-to-edge orientation (T-shaped). TMH 6 possesses the conserved Pro$^{6.50}$-Phe-Phe motif in both the adrenergic and serotoninergic subfamilies of GPCRs. It has been suggested that Phe$^{6.52}$ stabilizes the interaction of the aromatic catechol-containing ring with the β_2-adrenergic receptor[73] and the interaction with certain 5-HT$_{2A}$R ligands.[74] Near this recognition cavity are located two bulky residues: Val$^{3.33}$ and Ile$^{4.56}$. These residues are oriented toward the aromatic ring and thus limit the size of the recognition site. Thus, an interaction between the electron-rich clouds of the aromatic ring and the electron-poor hydrogens of the carbon atoms of Val$^{3.33}$ and Ile$^{4.56}$ is suggested. This type of C−H$\cdots\pi$ interaction plays a significant role in stabilizing local 3D structures of proteins.[75]

This optimized reduced model was used to position compound **56** inside the transmembrane domain of the 5-HT$_7$R (see Figure 4b). In addition to the described interactions, the NH group of the protonated piperazine ring of the ligand forms the frequently proposed ionic interaction with the O_δ atom of Asp$^{3.32}$ in the gauche+ side chain rotamer conformation (see Figure 4c). It is

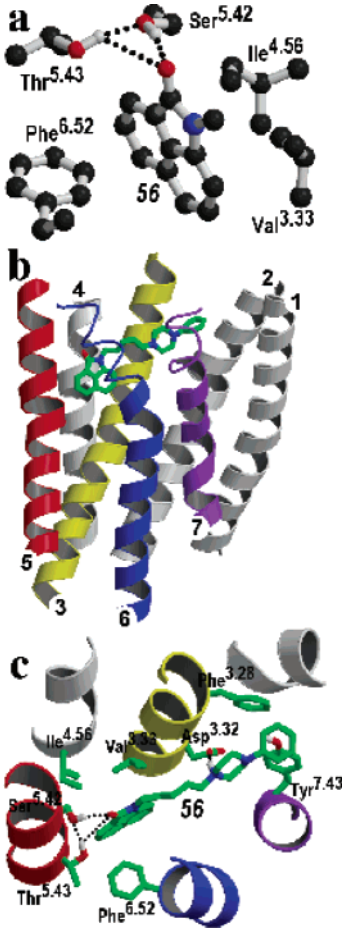

Figure 4. (a) Ab initio geometry optimization, with the ONIOM procedure, of compound **56** (the $-(CH_2)_5-$ chain plus the piperazine and phenyl rings were replaced by a methyl group) inside the side chains of Val$^{3.33}$, Ile$^{4.56}$, Ser$^{5.42}$, Thr$^{5.43}$, and Phe$^{6.52}$. Only polar hydrogens are depicted to offer a better view. (b) Molecular model of the complex between compound **56** and the transmembrane helix bundle of the 5-HT$_7$R constructed from the crystal structure of bovine rhodopsin, in a view parallel to the membrane. (c) Detailed view of the transmembrane helix bundle of the 5-HT$_7$R complexed with compound **56**. The carbonylic oxygen of the ligand is interacting with the hydroxyl groups of Ser$^{5.42}$ and Thr$^{5.43}$, the naphtholactam ring with Phe$^{6.52}$, the protonated piperazine ring with Asp$^{3.32}$, and the phenyl ring with Phe$^{3.28}$ and Tyr$^{7.43}$. Figures were created using MolScript v2.1.1[76] and Raster3D v2.5.[77]

important to remark that this gauche+ conformation differs from the trans conformation observed in our previous model of the 5-HT$_{1A}$R complexed with a piperazine derivative containing four methylene units as a spacer.[55] Thus, it seems reasonable to conclude that while the larger compound **56**, with five methylene units ($n = 5$), optimally interacts with Asp$^{3.32}$ pointing toward TMH 7 (*gauche*+), the shorter compound **51**, with four methylene units ($n = 4$), would optimally interact with Asp$^{3.32}$ pointing toward TMH 5 (trans). This finding provides a molecular explanation for the previous conclusion that the optimum spacer length is four or five methylene units. Finally, the phenyl ring attached to the piperazine ring expands between TMHs 3 and 7 and interacts with the aromatic side chains of Phe$^{3.28}$ and Tyr$^{7.43}$ (see Figure 4c).

Remarkably, the independent generation of a pharmacophore model and a 3D model of the transmembrane

domain of the 5-HT_7R complexed with ligand **56** have provided similar conclusions: (i) the HBA feature of the pharmacophore model binds $Ser^{5.42}$ and $Thr^{5.43}$; (ii) the HYD1 feature interacts with $Phe^{6.52}$; (iii) the PI feature forms an ionic interaction with $Asp^{3.32}$; and (iv) the HYD3 feature interacts with a set of aromatic residues ($Phe^{3.28}$, $Tyr^{7.43}$).

Conclusion

We present here an optimization of our postulated pharmacophore model for 5-HT_7R antagonism, by analyzing a variety of recently reported 5-HT_7R antagonists with the CATALYST program. The pharmacophore model consists of five features: a positive ionizable atom (PI), a H-bonding acceptor group (HBA), and three hydrophobic regions (HYD). To give support to the model, a series of new naphtholactam and naphthosultam derivatives of general structure **I** (**39**−**72**) were designed to interact with any or all pharmacophoric features simultaneously. This pharmacophore model was able to rationalize the relationships between the chemical features of synthesized compounds and their 5-HT_7R binding affinity data and confirmed that it incorporates the essential structural features for 5-HT_7R antagonism, thereby illustrating how the model can be used in the discovery of new classes of 5-HT_7R ligands. In addition, the independent generation of a 3D model of the transmembrane domain of the 5-HT_7R complexed with ligand **56** have provided similar conclusions: (i) the HBA feature of the pharmacophore model binds $Ser^{5.42}$ and $Thr^{5.43}$; (ii) the HYD1 feature interacts with $Phe^{6.52}$; (iii) the PI feature forms an ionic interaction with $Asp^{3.32}$; and (iv) the HYD3 (AR) feature interacts with a set of aromatic residues ($Phe^{3.28}$, $Tyr^{7.43}$). These results provide the tools for the design and synthesis of new ligands with predetermined affinities and pharmacological properties. Further synthesis and biological evaluation of new derivatives are currently in progress, and the results will be reported in due course.

Experimental Section

Chemistry. Melting points (uncorrected) were determined on a Gallenkamp electrothermal apparatus. Infrared (IR) spectra were obtained on a Perkin-Elmer 781 infrared spectrophotometer. ^1H and ^{13}C NMR spectra were recorded on a Varian VXR-300S, Bruker Avance 300, or Bruker AC-200 instrument. Chemical shifts (δ) are expressed in parts per million relative to internal tetramethylsilane; coupling constants (J) are in hertz. The following abbreviations are used to describe peak patterns when appropriate: s (singlet), d (doublet), t (triplet), q (quartet), qt (quintet), m (multiplet), br (broad). Elemental analyses (C, H, N) were determined at the UCM's analysis services and were within (±0.4% of the theoretical values. Analytical thin-layer chromatography (TLC) was run on Merck silica gel 60 F-254 plates with detection by UV light, iodine, acidic vanillin solution, or 10% phosphomolybdic acid solution in ethanol. For normal pressure and flash chromatography, Merck silica gel type 60 (size 70−230 and 230−400 mesh, respectively) was used. Unless stated otherwise, starting materials and reagents used were high-grade commercial products purchased from Aldrich, Fluka, or Merck. All solvents were distilled prior to use. Dry DMF was obtained by stirring with CaH_2 followed by distillation under argon. All final compounds (**39**−**72**) were prepared as hydrochloride salts for biological assays, and spectral data refer to free bases.

The following intermediates were synthesized according to described procedures: 1-(3-chloropropyl)-4-phenylpiperazine (**73**),[78] 1-(3-chloropropyl)-4-(2-methoxyphenyl)piperazine (**74**),[78] 4-isopropylpiperidine (**81**),[79] 4-cyclohexylpiperidine (**82**),[80] and 4-phenylpiperidine (**83**).[81] Spectral data of all described compounds were consistent with the proposed structures for series **75**−**80** and **39**−**72**; here we include the data of compounds **75**, **78**, **39**, **42**, **45**, **48**, **50**, **56**, **58**, **63** and **72**.

Synthesis of 1-(ω-Bromoalkyl)benzo[*cd*]indol-2(1*H*)-ones and 2-(ω-Bromoalkyl)-2*H*-naphtho[1,8-*cd*]isothiazole 1,1-Dioxides 75−80. General Procedure. To a solution of benzo[*cd*]indol-2(1*H*)-one or 2*H*-naphtho[1,8-*cd*]isothiazole 1,1-dioxide (26 mmol) in anhydrous DMF (30 mL) was added NaH 60% (1.0 g, 26 mmol). After stirring for 1 h at 60 °C under an argon atmosphere, a solution of the corresponding dibromoalkyl derivative (52 mmol) in anhydrous DMF (25 mL) was added. The mixture was refluxed under argon at 110 °C for 3 h (TLC). Then, the solvent was evaporated under reduced pressure, and the residue was resuspended in water (50 mL) and extracted with dichloromethane (3 × 50 mL). The combined organic layers were washed with water and dried over anhydrous $MgSO_4$. After evaporation of the solvent, the crude oil was purified by column chromatography to afford the desired derivatives **75**−**80** as pure compounds (eluents, hexane/ethyl acetate; relative proportions depending upon the compound). In all cases, small amounts of the dialkylated compound (25−35%) and starting material (5−10%) were observed in the ^1H NMR spectra of the reaction crudes.

1-(4-Bromobutyl)benzo[*cd*]indol-2(1*H*)-one (75): yield 5.2 g (65%); chromatography hexane/ethyl acetate, from 13:1 to 1:1; mp 80−82 °C (chloroform/ hexane); ^1H NMR ($CDCl_3$) δ 1.96 (qt, J = 7.2, 4H), 3.46 (t, J = 6.6, 2H), 3.96 (t, J = 6.2, 2H), 6.92 (d, J = 6.8, 1H), 7.46 (dd, J = 8.4, 6.9, 1H), 7.53 (d, J = 8.4, 1H), 7.70 (dd, J = 8.1, 6.9, 1H), 8.00 (d, J = 8.2, 1H), 8.05 (d, J = 6.9, 1H); ^{13}C NMR ($CDCl_3$) δ 27.4, 29.9, 33.9, 39.3, 105.1, 120.5, 124.4, 125.2, 126.6, 128.6, 128.8, 129.2, 130.9, 139.3, 168.2.

1-(5-Bromopentyl)benzo[*cd*]indol-2(1*H*)-one (76): yield 4.4 g (53%); chromatography hexane/ethyl acetate, from 13:1 to 1:1; bp 289−292 °C/0.06 mmHg.

1-(6-Bromohexyl)benzo[*cd*]indol-2(1*H*)-one (77): yield 4.4 g (50%); chromatography hexane/ethyl acetate, from 13:1 to 1:1; bp 177−180 °C/0.06 mmHg.

2-(4-Bromobutyl)-2*H*-naphtho[1,8-*cd*]isothiazole 1,1-dioxide (78): yield 5.4 g (61%); chromatography hexane/ethyl acetate, 8.5:1.5; mp 67−69 °C (chloroform/hexane); ^1H NMR ($CDCl_3$) δ 2.06−2.12 (m, 4H), 3.49 (t, J = 7.6, 2H), 3.88 (t, J = 6.8, 2H), 6.76 (dd, J = 7.1, 1.0, 1H), 7.46 (dd, J = 8.5, 1.0, 1H), 7.55 (dd, J = 8.5, 7.1, 1H), 7.75 (dd, J = 8.1, 7.3, 1H), 7.97 (dd, J = 7.3, 0.7, 1H), 8.07 (dd, J = 8.1, 0.7, 1H); ^{13}C NMR ($CDCl_3$) δ 26.6, 29.7, 32.9, 41.1, 102.8, 118.1, 119.1, 119.7, 128.0, 129.2, 130.1, 130.6, 131.1, 136.3.

2-(5-Bromopentyl)-2*H*-naphtho[1,8-*cd*]isothiazole 1,1-dioxide (79): yield 5.3 g (58%); chromatography hexane/ethyl acetate, 9:1; mp 62−64 °C (chloroform/hexane).

2-(6-Bromohexyl)-2*H*-naphtho[1,8-*cd*]isothiazole 1,1-dioxide (80): yield 4.2 g (44%); chromatography hexane/ethyl acetate, from 9:1 to 8:2; mp 67−69 °C (chloroform/hexane).

General Method A. Preparation of Derivatives 39, 40. To a suspension of benzo[*cd*]indol-2(1*H*)-one (0.5 g, 3 mmol) and 0.23 mL (3 mmol) of 35% formaldehyde in 7 mL of ethanol was added the corresponding 1-arylpiperazine (3 mmol) and was refluxed for 1−4 h (TLC). The reaction mixture was allowed to cool, then the solvent was evaporated under reduced pressure, and the residue was resuspended in water (20 mL) and extracted with chloroform (3 × 20 mL). The combined organic layers were dried over anhydrous Na_2SO_4. After evaporation of the solvent, the crude oil was purified by column chromatography (eluent, hexane/ethyl acetate; relative proportions depending upon the compound).

1-[(4-Phenylpiperazin-1-yl)methyl]benzo[*cd*]indol-2(1*H*)-one (39): yield 0.7 g (69%); chromatography hexane/ethyl acetate, from 8:2 to 1:1; mp 153−155 °C (chloroform/hexane); ^1H NMR ($CDCl_3$) δ 2.88 (t, J = 5.1, 4H), 3.18 (t, J = 5.1, 4H), 4.79 (s, 2H), 6.80 (t, J = 7.2, 1H), 6.86 (d, J = 7.8, 2H), 7.07 (d, J = 6.9, 1H), 7.18−7.26 (m, 2H), 7.46 (dd, J = 8.4, 6.9, 1H), 7.55 (d, J = 8.4, 1H), 7.72 (dd, J = 8.7, 7.2, 1H),

8.03 (d, $J = 7.8$, 1H), 8.08 (d, $J = 6.9$, 1H); ^{13}C NMR ($CDCl_3$) δ 49.0, 50.6, 61.9, 106.0, 116.1, 119.6, 120.2, 124.6, 125.1, 126.1, 128.3, 128.5, 128.9, 129.0, 130.9, 139.9, 151.1, 168.7. Anal. ($C_{22}H_{21}N_3O\cdot 2HCl\cdot {}^3/_2H_2O$) C, H, N.

1-{[4-(2-Methoxyphenyl)piperazin-1-yl]methyl}benzo[*cd*]indol-2(1*H*)-one (40): yield 1.0 g (88%); chromatography hexane/ethyl acetate, 1:1; mp 160−163 °C (chloroform/hexane). Anal. ($C_{23}H_{23}N_3O_2\cdot 2HCl\cdot 3H_2O$) C, H, N.

General Method B. Preparation of Derivatives 41, 42. To a solution of benzo[*cd*]indol-2(1*H*)-one (1.0 g, 6 mmol) in anhydrous DMF (3.3 mL) was added slowly 60% NaH (0.25 g, 6 mmol), and the mixture was warmed at 60 °C for 1 h under an argon atmosphere. Then, a solution of the corresponding 1-aryl-4-(3-chloropropyl)piperazine **73**, **74** (6 mmol) in anhydrous DMF (3.3 mL) was added dropwise and the mixture was refluxed at 110 °C under argon for 1−3 h (TLC). The solvent was evaporated under reduced pressure, the residue was resuspended in water (50 mL) and extracted with dichloromethane (3 × 50 mL). The combined organic layers were dried over anhydrous Na_2SO_4. After evaporation of the solvent, the crude oil was purified by column chromatography (eluent, hexane/ethyl acetate; relative proportions depending upon the compound).

1-[3-(4-Phenylpiperazin-1-yl)propyl]benzo[*cd*]indol-2(1*H*)-one (41): yield 1.4 g (64%); chromatography hexane/ethyl acetate, 2:8; mp 192−195 °C (chloroform/diethyl ether). Anal. ($C_{24}H_{25}N_3O\cdot 2HCl\cdot {}^5/_2H_2O$) C, H, N.

1-{3-[4-(2-Methoxyphenyl)piperazin-1-yl]propyl}benzo[*cd*]indol-2(1*H*)-one (42): yield 1.7 g (72%); chromatography hexane/ethyl acetate, 7:3; mp 200−202 °C (chloroform/diethyl ether); ^{1}H NMR ($CDCl_3$) δ 1.26 (qt, $J = 7.1$, 2H), 2.52 (t, $J = 7.1$, 2H), 2.62 (br s, 4H), 3.05 (br s, 4H), 3.85 (s, 3H), 4.02 (t, $J = 6.8$, 2H), 6.83−7.05 (m, 5H), 7.44 (dd, $J = 8.5$, 6.6, 1H), 7.55 (dd, $J = 8.5$, 1.0, 1H), 7.71 (dd, $J = 8.4$, 6.8, 1H), 8.00 (d, $J = 8.0$, 1H), 8.04 (d, $J = 6.8$, 1H); ^{13}C NMR ($CDCl_3$) δ 25.9, 38.4, 50.6, 53.3, 55.3, 55.5, 105.1, 111.2, 118.0, 120.1, 120.9, 122.8, 124.1, 125.9, 126.7, 128.4, 128.6, 129.1, 130.7, 139.7, 141.3, 152.2, 168.9. Anal. ($C_{25}H_{27}N_3O_2\cdot 2HCl\cdot {}^7/_2H_2O$) C, H, N.

General Method C. Preparation of Derivatives 43−71. To a suspension of the corresponding derivatives **75**−**80** (9 mmol) and the appropriate amine (15 mmol) in acetonitrile (19 mL) was added 2.0 mL of triethylamine (1.5 g, 15 mmol), and the mixture was stirred at 60 °C for 18−24 h (TLC). Then, the solvent was evaporated under reduced pressure and the residue was resuspended in water and extracted with dichloromethane (3 × 100 mL). The combined organic layers were dried over anhydrous Na_2SO_4. After evaporation of the solvent, the crude oil was purified by column chromatography (eluent, hexane/ethyl acetate, ethyl acetate/ethanol, or chloroform/methanol; relative proportions depending upon the compound).

1-(4-Piperidinobutyl)benzo[*cd*]indol-2(1*H*)-one (43): yield 2.5 g (89%); chromatography chloroform/methanol, 9:1; mp 198−200 °C (chloroform/hexane). Anal. ($C_{20}H_{24}N_2O\cdot HCl\cdot 2H_2O$) C, H, N.

1-[4-(4-Methylpiperidino)butyl]benzo[*cd*]indol-2(1*H*)-one (44): yield 1.7 g (60%); chromatography ethyl acetate/ethanol, 7:3; mp 204−207 °C (chloroform/hexane). Anal. ($C_{21}H_{26}N_2O\cdot HCl\cdot 2H_2O$) C, H, N.

1-[4-(4-Isopropylpiperidino)butyl]benzo[*cd*]indol-2(1*H*)-one (45): yield 2.7 g (84%); chromatography ethyl acetate/ethanol, 8:2; mp 173−175 °C (chloroform/diethyl ether); ^{1}H NMR ($CDCl_3$) δ 0.79 (d, $J = 6.7$, 6H), 0.85−1.00 (m, 1H), 1.12−1.45 (m, 3H), 1.51−1.91 (m, 8H), 2.34 (t, $J = 7.5$, 2H), 2.91 (d, $J = 11.4$, 2H), 3.88 (t, $J = 7.1$, 2H), 6.86 (d, $J = 6.6$, 1H), 7.39 (dd, $J = 8.5$, 6.6, 1H), 7.47 (d, $J = 8.4$, 1H), 7.64 (dd, $J = 8.1$, 7.1, 1H), 7.95 (d, $J = 8.5$, 1H), 7.98 (d, $J = 7.2$, 1H); ^{13}C NMR ($CDCl_3$) δ 19.8, 24.1, 26.8, 29.0, 32.4, 40.0, 42.3, 54.3, 58.3, 105.1, 120.2, 124.2, 125.4, 126.9, 128.5, 128.6, 129.2, 130.8, 139.5, 168.2. Anal. ($C_{23}H_{30}N_2O\cdot HCl\cdot {}^1/_2H_2O$) C, H, N.

1-[4-(4-Cyclohexylpiperidino)butyl]benzo[*cd*]indol-2(1*H*)-one (46): yield 2.7 g (78%); chromatography ethyl acetate/ethanol, 9:1; mp 217−219 °C (chloroform/hexane). Anal. ($C_{26}H_{34}N_2O\cdot HCl\cdot {}^1/_2H_2O$) C, H, N.

1-[4-(4-Phenylpiperidino)butyl]benzo[*cd*]indol-2(1*H*)-one (47): yield 2.3 g (66%); chromatography hexane/ethyl acetate, from 1:1 to ethyl acetate; mp 215−217 °C (chloroform/diethyl ether). Anal. ($C_{26}H_{28}N_2O\cdot HCl\cdot 2H_2O$) C, H, N.

1-[4-(4-Phenyl-3,6-dihydropyridin-1(2*H*)-yl)butyl]benzo[*cd*]indol-2(1*H*)-one (48): yield 1.6 g (54%); chromatography hexane/ethyl acetate, from 3:7 to ethyl acetate; mp 222−224 °C (dec) (chloroform/hexane); ^{1}H NMR ($CDCl_3$) δ 1.68 (qt, $J = 8.4$, 2H), 1.86 (qt, $J = 7.5$, 2H), 2.46−2.54 (m, 4H), 2.67 (t, $J = 7.5$, 2H), 3.12 (d, $J = 3.3$, 2H), 3.97 (t, $J = 7.2$, 2H), 6.03 (t, $J = 1.8$, 1H), 6.93 (d, $J = 6.9$, 1H), 7.21−7.34 (m, 5H), 7.46 (td, $J = 8.4$, 1.8, 1H), 7.52 (d, $J = 8.1$, 1H), 7.70 (ddd, $J = 8.1$, 6.9, 1.8, 1H), 8.00 (d, $J = 8.1$, 1H), 8.04 (d, $J = 6.9$, 1H); ^{13}C NMR ($CDCl_3$) δ 24.5, 26.8, 28.1, 40.1, 50.4, 53.3, 57.8, 105.1, 120.3, 121.8, 124.3, 125.0, 125.3, 126.8, 127.0, 128.3, 128.5, 128.7, 129.6, 130.8, 135.0, 139.5, 140.9, 168.2. Anal. ($C_{26}H_{26}N_2O\cdot HCl\cdot {}^1/_2H_2O$) C, H, N.

1-[4-(4-Methylpiperazin-1-yl)butyl]benzo[*cd*]indol-2(1*H*)-one (49): yield 2.2 g (76%); chromatography chloroform/methanol, 6:4; mp 268−270 °C (dec) (chloroform/hexane). Anal. ($C_{20}H_{25}N_3O\cdot 2HCl\cdot {}^1/_2H_2O$) C, H, N.

1-[4-(4-Cyclohexylpiperazin-1-yl)butyl]benzo[*cd*]indol-2(1*H*)-one (50): yield 3.2 g (90%); chromatography ethyl acetate; mp 290−292 °C (dec) (chloroform/diethyl ether); ^{1}H NMR ($CDCl_3$) δ 1.00−1.27 (m, 5H), 1.55−1.62 (m, 3H), 1.75−1.83 (m, 4H), 1.90−1.92 (m, 2H), 2.30−2.41 (m, 3H), 2.54 (br s, 4H), 2.66 (br s, 4H), 3.91 (t, $J = 6.9$, 2H), 6.88 (d, $J = 6.9$, 1H), 7.42 (dd, $J = 8.4$, 6.9, 1H), 7.50 (d, $J = 8.4$, 1H), 7.67 (dd, $J = 8.1$, 7.2, 1H), 7.98 (d, $J = 8.4$, 1H), 8.02 (d, $J = 6.9$, 1H); ^{13}C NMR ($CDCl_3$) δ 24.3, 26.0, 26.3, 26.9, 28.9, 40.2, 48.9, 53.3, 58.1, 63.9, 105.2, 120.3, 124.4, 125.3, 126.9, 128.6, 128.8, 129.3, 130.9, 139.6, 168.2. Anal. ($C_{25}H_{33}N_3O\cdot 2HCl\cdot {}^5/_2H_2O$) C, H, N.

1-[4-(4-Phenylpiperazin-1-yl)butyl]benzo[*cd*]indol-2(1*H*)-one (51): yield 3.0 g (86%); chromatography ethyl acetate; mp 255−257 °C (dec) (dichloromethane/hexane). Anal. ($C_{25}H_{27}N_3O\cdot 2HCl\cdot H_2O$) C, H, N.

1-{4-[4-(2-Methoxyphenyl)piperazin-1-yl]butyl}benzo[*cd*]indol-2(1*H*)-one (52): yield 3.0 g (80%); chromatography ethyl acetate; mp 219−221 °C (dec) (chloroform/hexane). Anal. ($C_{26}H_{29}N_3O_2\cdot 2HCl$) C, H, N.

1-[5-(4-Isopropylpiperidino)pentyl]benzo[*cd*]indol-2(1*H*)-one (53): yield 2.7 g (83%); chromatography ethyl acetate/ethanol, 8:2; mp 212−215 °C (acetone/ diethyl ether). Anal. ($C_{24}H_{32}N_2O\cdot HCl$) C, H, N.

1-[5-(4-Phenyl-3,6-dihydropyridin-1(2*H*)-yl)pentyl]benzo[*cd*]indol-2(1*H*)-one (54): yield 1.9 g (53%); chromatography hexane/ethyl acetate, 1:1; bp 230−232 °C/0.06 mmHg. Anal. ($C_{27}H_{28}N_2O\cdot HCl\cdot {}^3/_2H_2O$) C, H, N.

1-[5-(4-Cyclohexylpiperazin-1-yl)pentyl]benzo[*cd*]indol-2(1*H*)-one (55): yield 3.3 g (91%); chromatography ethyl acetate; mp 259−261 °C (dec) (chloroform/diethyl ether). Anal. ($C_{26}H_{35}N_3O\cdot 2HCl\cdot {}^3/_2H_2O$) C, H, N.

1-[5-(4-Phenylpiperazin-1-yl)pentyl]benzo[*cd*]indol-2(1*H*)-one (56): yield 3.3 g (93%); chromatography ethyl acetate; mp 211−213 °C (dichloromethane/hexane); ^{1}H NMR ($CDCl_3$) δ 1.43 (qt, $J = 7.2$, 2H), 1.58 (qt, $J = 7.5$, 2H), 1.82 (qt, $J = 7.5$, 2H), 2.35 (t, $J = 7.5$, 2H), 2.55 (t, $J = 5.1$, 4H), 3.15 (t, $J = 5.1$, 4H), 3.92 (t, $J = 7.5$, 2H), 6.83 (t, $J = 7.2$, 1H), 6.87−6.93 (m, 3H), 7.24 (t, $J = 6.9$, 2H), 7.45 (dd, $J = 8.4$, 6.9, 1H), 7.52 (d, $J = 8.4$, 1H), 7.69 (dd, $J = 8.1$, 6.9, 1H), 7.99 (d, $J = 6.9$, 1H), 8.04 (d, $J = 7.2$, 1H); ^{13}C NMR ($CDCl_3$) δ 24.8, 26.5, 28.6, 40.1, 49.0, 53.2, 58.4, 104.8, 115.9, 119.5, 120.1, 124.1, 125.1, 126.7, 128.4, 128.6, 129.0, 129.6, 130.6, 139.5, 151.2, 168.0. Anal. ($C_{26}H_{29}N_3O\cdot 2HCl$) C, H, N.

1-{5-[4-(2-Methoxyphenyl)piperazin-1-yl]pentyl}benzo[*cd*]indol-2(1*H*)-one (57): yield 2.9 g (75%); chromatography ethyl acetate; mp 209−211 °C (chloroform/hexane). Anal. ($C_{27}H_{31}N_3O_2\cdot 2HCl\cdot {}^1/_2H_2O$) C, H, N.

1-[6-(4-Phenylpiperazin-1-yl)hexyl]benzo[*cd*]indol-2(1*H*)-one (58): yield 3.0 g (80%); chromatography ethyl acetate; mp 183−185 °C (chloroform/diethyl ether); ^{1}H NMR ($CDCl_3$) δ 1.30−1.61 (m, 6H), 1.81 (qt, $J = 7.1$, 2H), 2.39 (t, $J = 6.8$, 2H), 2.60 (t, $J = 5.1$, 4H), 3.20 (t, $J = 5.1$, 4H), 3.93 (t, $J = 7.3$, 2H), 6.81−6.97 (m, 4H), 7.26 (t, $J = 7.3$, 2H), 7.46

(dd, J = 8.5, 6.6, 1H), 7.54 (dd, J = 8.3, 1.0, 1H), 7.71 (dd, J = 8.3, 6.8, 1H), 8.02 (dd, J = 8.3, 0.7, 1H), 8.06 (dd, J = 6.8, 0.7, 1H); ^{13}C NMR ($CDCl_3$) δ 26.8, 27.0, 27.4, 28.9, 40.4, 49.1, 53.3, 58.7, 105.1, 116.2, 119.8, 120.3, 124.4, 125.3, 126.9, 128.6, 128.8, 129.2, 129.4, 130.9, 139.7, 151.4, 168.2. Anal. ($C_{27}H_{31}N_3O\cdot 2HCl\cdot 2H_2O$) C, H, N.

1-{6-[4-(2-Methoxyphenyl)piperazin-1-yl]hexyl}benzo[*cd*]indol-2(1*H*)-one (59): yield 3.8 g (94%); chromatography ethyl acetate; mp 188−190 °C (chloroform/hexane). Anal. ($C_{28}H_{33}N_3O_2\cdot HCl\cdot H_2O$) C, H, N.

2-(4-Piperidinobutyl)-2*H*-naphtho[1,8-*cd*]isothiazole 1,1-dioxide (60): yield 2.8 g (89%); chromatography chloroform/methanol, 9:1; mp 217−219 °C (chloroform/hexane). Anal. ($C_{19}H_{24}N_2O_2S\cdot HCl$) C, H, N.

2-[4-(4-Methylpiperidino)butyl]-2*H*-naphtho[1,8-*cd*]isothiazole 1,1-dioxide (61): yield 2.8 g (87%); chromatography chloroform/methanol, 9:1; mp 219−221 °C (dec) (chloroform/hexane). Anal. ($C_{20}H_{26}N_2O_2S\cdot HCl$) C, H, N.

2-[4-(4-Methylpiperazin-1-yl)butyl]-2*H*-naphtho[1,8-*cd*]isothiazole 1,1-dioxide (62): yield 2.6 g (81%); chromatography chloroform/methanol, from 9.5:0.5 to 9:1; mp 265−268 °C (dec) (chloroform/hexane). Anal. ($C_{19}H_{25}N_3O_2S\cdot 2HCl\cdot {}^1/_2H_2O$) C, H, N.

2-[4-(4-Phenylpiperazin-1-yl)butyl]-2*H*-naphtho[1,8-*cd*]isothiazole 1,1-dioxide (63): yield 3.1 g (81%); chromatography hexane/ethyl acetate, from 1:1 to ethyl acetate; mp 213-215 °C (dichloromethane/hexane); ^{1}H NMR ($CDCl_3$) δ 1.72 (qt, J = 7.5, 2H), 1.98 (qt, J = 7.5, 2H), 2.47 (t, J = 7.5, 2H), 2.59 (t, J = 4.8, 4H), 3.18 (t, J = 4.8, 4H), 3.86 (t, J = 7.5, 2H), 6.75 (d, J = 6.9, 1H), 6.83 (t, J = 7.5, 1H), 6.90 (d, J = 7.8, 2H), 7.25 (t, J = 7.2, 2H), 7.43 (d, J = 8.4, 1H), 7.52 (dd, J = 8.4, 7.2, 1H), 7.73 (dd, J = 8.1, 7.2, 1H), 7.94 (d, J = 7.2, 1H), 8.05 (d, J = 8.4, 1H); ^{13}C NMR ($CDCl_3$) δ 24.1, 26.1, 42.0, 49.1, 53.2, 57.8, 102.9, 116.0, 118.1, 119.3, 119.6, 119.7, 128.0, 129.0, 129.3, 130.4, 130.7, 131.1, 136.6, 151.3. Anal. ($C_{24}H_{27}N_3O_2S\cdot 2HCl\cdot {}^1/_2H_2O$) C, H, N.

2-{4-[4-(2-Methoxyphenyl)piperazin-1-yl]butyl}-2*H*-naphtho[1,8-*cd*]isothiazole 1,1-dioxide (64): yield 3.3 g (82%); chromatography ethyl acetate; mp 211−213 °C (dichloromethane/diethyl ether). Anal. ($C_{25}H_{29}N_3O_3S\cdot 2HCl$) C, H, N.

2-[5-(4-Methylpiperidino)pentyl]-2*H*-naphtho[1,8-*cd*]isothiazole 1,1-dioxide (65): yield 3.3 g (98%); chromatography chloroform/methanol, 9:1; mp 187−189 °C (chloroform). Anal. ($C_{21}H_{28}N_2O_2S\cdot 2HCl\cdot {}^5/_2H_2O$) C, H, N.

2-[5-(4-Cyclohexylpiperidino)pentyl]-2*H*-naphtho[1,8-*cd*]isothiazole 1,1-dioxide (66): yield 3.9 g (98%); chromatography ethyl acetate/ethanol, 9:1; mp 163−165 °C (methanol/diethyl ether). Anal. ($C_{26}H_{36}N_2O_2S\cdot HCl\cdot H_2O$) C, H, N.

2-[5-(4-Phenylpiperazin-1-yl)pentyl]-2*H*-naphtho[1,8-*cd*]isothiazole 1,1-dioxide (67): yield 3.7 g (94%); chromatography hexane/ethyl acetate, from 3:7 to 1:9; mp 216−218 °C (dichloromethane/hexane). Anal. ($C_{25}H_{29}N_3O_2S\cdot 2HCl$) C, H, N.

2-{5-[4-(2-Methoxyphenyl)piperazin-1-yl]pentyl}-2*H*-naphtho[1,8-*cd*]isothiazole 1,1-dioxide (68): yield 3.7 g (87%); chromatography ethyl acetate/ethanol, 8:2; mp 210−212 °C (methanol/diethyl ether). Anal. ($C_{26}H_{31}N_3O_3S\cdot 2HCl$) C, H, N.

2-[6-(4-Methylpiperidino)hexyl]-2*H*-naphtho[1,8-*cd*]isothiazole 1,1-dioxide (69): yield 3.2 g (93%); chromatography ethyl acetate/ethanol, from 8.5:1.5 to 8:2; mp 168−170 °C (chloroform/hexane). Anal. ($C_{22}H_{30}N_2O_2S\cdot HCl\cdot 3H_2O$) C, H, N.

2-[6-(4-Phenylpiperazin-1-yl)hexyl]-2*H*-naphtho[1,8-*cd*]isothiazole 1,1-dioxide (70): yield 3.4 g (84%); chromatography hexane/ethyl acetate, from 4:6 to ethyl acetate; mp 205−207 °C (chloroform/diethyl ether). Anal. ($C_{26}H_{31}N_3O_2S\cdot 2HCl$) C, H, N.

2-{6-[4-(2-Methoxyphenyl)piperazin-1-yl]hexyl}-2*H*-naphtho[1,8-*cd*]isothiazole 1,1-dioxide (71): yield 3.5 g (80%); chromatography ethyl acetate; mp 203−205 °C (chloroform/hexane). Anal. ($C_{27}H_{33}N_3O_3S\cdot 2HCl$) C, H, N.

Synthesis of 1-{4-[(1-Methyl-1*H*-imidazol-2-yl)thio]butyl}benzo[*cd*]indol-2(1*H*)-one (72). To a solution of sodium methoxide (0.7 g, 13 mmol) in 20 mL of methanol chilled to 0 °C was added 1-methyl-1*H*-imidazole-2-thiol (1.5 g, 13 mmol). After 5 min, compound **75** (4.0 g, 13 mmol) was added in one portion, and the mixture was stirred and allowed to come to room temperature overnight. The solution was diluted with 30 mL of water and extracted with diethyl ether (3 × 50 mL). The combined organic extracts were washed with 10% NaOH, water, and brine and dried over anhydrous Na_2SO_4. After evaporation of the solvent, the crude oil was purified by column chromatography (hexane/ethyl acetate, from 1:1 to 0.5:9.5) to afford 3.4 g (77%) of **72**: mp 181−183 °C; ^{1}H NMR ($CDCl_3$) δ 1.72−2.00 (m, 4H), 3.09 (t, J = 6.8, 2H), 3.57 (s, 3H), 3.93 (t, J = 6.8, 2H), 6.87 (d, J = 1.5, 1H), 6.91 (dd, J = 6.6, 0.7, 1H), 7.01 (d, J = 1.2, 1H), 7.45 (dd, J = 8.5, 6.6, 1H), 7.53 (dd, J = 8.5, 0.7, 1H), 7.70 (dd, J = 8.3, 6.8, 1H), 8.01 (d, J = 7.6, 1H), 8.05 (d, J = 7.1, 1H); ^{13}C NMR ($CDCl_3$) δ 27.3, 27.8, 33.3, 34.0, 39.8, 105.2, 120.4, 122.3, 124.4, 125.3, 126.8, 128.7, 128.8, 129.3, 129.4, 130.9, 139.5, 141.7, 168.2. Anal. ($C_{19}H_{19}N_3OS\cdot HCl$) C, H, N.

Radioligand Binding Assays at 5-HT$_7$R. Male Sprague−Dawley rats (*Rattus norvegicus albinus*), weighing 180−200 g, were killed by decapitation and the brains rapidly removed and dissected. The receptor binding studies were performed by a modification of a previously described procedure.[68] The hypothalamus was homogenized in 5 mL of ice-cold Tris buffer (50 mM Tris-HCl, pH 7.4 at 25 °C) and centrifuged at 48 000*g* for 10 min. The membrane pellet was washed by resuspension and centrifugation, and then the resuspended pellet was incubated at 37 °C for 10 min. Membranes were then collected by centrifugation, and the final pellet was resuspended in 100 volumes of ice-cold 50 mM Tris-HCl, 4 mM $CaCl_2$, 1 mg/mL ascorbic acid, 0.01 mM pargyline, and 3 μM pindolol[82] buffer (pH 7.4 at 25 °C). Fractions of 400 μL of the final membrane suspension were incubated at 23 °C for 120 min. with 0.5 nM [^{3}H]-5-CT (88 Ci/mmol), in the presence or absence of several concentrations of the competing drug, in a final volume of 0.5 mL of assay buffer (50 mM Tris-HCl, 4 mM $CaCl_2$, 1 mg/mL ascorbic acid, 0.01 mM pargyline, and 3 μM pindolol buffer (pH 7.4 at 25 °C)). Nonspecific binding was determined with 10 μM 5-HT. Competing drug, nonspecific, total, and radioligand bindings were defined in triplicate. Incubation was terminated by rapid vacuum filtration through Whatman GF/C filters, presoaked in 0.01% poly(ethylenimine), using a Brandel cell harvester. The filters were then washed with the assay buffer and were placed in vials to which were added 4 mL of a scintillation cocktail (Ecolite), and the radioactivity bound to the filters was measured by liquid scintillation spectrometry. The data were analyzed by an iterative curve-fitting procedure (program Prism Graph Pad), which provided IC_{50}, K_i, and r^2 values for test compounds, K_i values being calculated from the Cheng−Prusoff equation.[69] The protein concentrations of the rat hypothalamus were determined by the method of Lowry,[83] using bovine serum albumin as the standard.

Acknowledgment. This work was supported by Ministerio de Ciencia y Tecnología (BQU2001-1457). The authors are grateful to U.N.E.D. for a predoctoral grant to E. Porras.

Supporting Information Available: Spectral data of new intermediates **76**, **77**, **79**, and **80** and final compounds **40**, **41**, **43**, **44**, **46**, **47**, **49**, **51**−**55**, **57**, **59**−**62**, and **64**−**71**. This material is available free of charge via the Internet at http://pubs.acs.org.

References

(1) *Serotoninergic Neurons and 5-HT Receptors in the CNS*; Baumgarten, H. G., Göthert, M., Eds.; Springer-Verlag: Berlin, 1997.
(2) Olivier, B.; van Wijngaarden, I.; Soudijn, W. *Serotonin Receptors and their Ligands*; Olivier, B., van Wijngaarden, I., Soudijn, W., Eds.; Elsevier: The Netherlands, 1997.
(3) Barnes, N. M.; Sharp, T. A Review of Central 5-HT Receptors and their Function. *Neuropharmacology* **1999**, *38*, 1083−1152.
(4) Hoyer, D.; Hannon, J. P.; Martin, G. R. Molecular, Pharmacological and Functional Diversity of 5-HT Receptors. *Pharmacol. Biochem. Behav.* **2002**, *71*, 533−554.

(5) Bikker, J. A.; Trumpp-Kallmeyer, S.; Humblet, C. G-Protein Coupled Receptors: Models, Mutagenesis, and Drug Design. *J. Med. Chem.* **1998**, *41*, 2911−2927.
(6) Klabunde, T.; Hessler, G. Drug Design Strategies for Targeting G-Protein-Coupled Receptors. *ChemBioChem.* **2002**, *3*, 928−944.
(7) Eglen, R. M.; Jasper, J. R.; Chang, D. J.; Martin, G. R. The 5-HT_7 Receptor: Orphan Found. *Trends Pharmacol. Sci.* **1997**, *18*, 104−107.
(8) Vanhoenacker, P.; Haegeman, G.; Leysen, J. E. 5-HT_7 Receptors: Current Knowledge and Future Prospects. *Trends Pharmacol. Sci.* **2000**, *21*, 70−77.
(9) Lovenberg, T. W.; Baron, B. M.; de Lecea, L.; Miller, J. D.; Prosser, R. A.; Rea, M. A.; Foye, P. E.; Racke, M.; Slone, A. L.; Siegel, B. W.; Danielson, P. E.; Sutcliffe, J. G.; Erlander, M. G. A Novel Adenylyl Cyclase-Activating Serotonin Receptor (5-HT_7) Implicated in the Regulation of Mammalian Circadian Rhythms. *Neuron* **1993**, *11*, 449−458.
(10) Plassat, J.-L.; Amlaiky, N.; Hen, R. Molecular Cloning of a Mammalian Serotonin Receptor that Activates Adenylate Cyclase. *Mol. Pharmacol.* **1993**, *44*, 229−236.
(11) Ruat, M.; Traiffort, E.; Leurs, R.; Tardivel-Lacombe, J.; Diaz, J.; Arrang, J.-M.; Schwartz, J.-C. Molecular Cloning, Characterization, and Localization of a High-Affinity Serotonin Receptor (5-HT_7) Activating cAMP Formation. *Proc. Natl. Acad. Sci. U.S.A.* **1993**, *90*, 8547−8551.
(12) Shen, Y.; Monsma, F. J., Jr.; Metcalf, M. A.; Jose, P. A.; Hamblin, M. W.; Sibley, D. R. Molecular Cloning and Expression of a 5-Hydroxytryptamine$_7$ Serotonin Receptor Subtype. *J. Biol. Chem.* **1993**, *268*, 18200−18204.
(13) Tsou, A.-P.; Kosaka, A.; Bach, C.; Zuppan, P.; Yee, C.; Tom, L.; Alvarez, R.; Ramsey, S.; Bonhaus, D. W.; Stefanich, E.; Jakeman, L.; Eglen, R. M.; Chan, H. W. Cloning and Expression of a 5-Hydroxytryptamine$_7$ Receptor Positively Coupled to Adenylyl Cyclase. *J. Neurochem.* **1994**, *63*, 456−464.
(14) Bard, J. A.; Zgombick, J.; Adham, N.; Vaysse, P.; Branchek, T. A.; Weinshank, R. L. Cloning of a Novel Human Serotonin Receptor (5-HT_7) Positively Linked to Adenylate Cyclase. *J. Biol. Chem.* **1993**, *268*, 23422−23426.
(15) Heidmann, D. E. A.; Metcalf, M. A.; Kohen, R.; Hamblin, M. W. Four 5-Hydroxytryptamine$_7$ (5-HT_7) Receptor Isoforms in Human and Rat Produced by Alternative Splicing: Species Differences Due to Altered Intron-Exon Organization. *J. Neurochem.* **1997**, *68*, 1372−1381.
(16) Liu, H.; Irving, R. H.; Coupar, I. M. Expression Patterns of 5-HT_7 Receptor Isoforms in the Rat Digestive Tract. *Life Sci.* **2001**, *69*, 2467−2475.
(17) Krobert, K. A.; Levy, F. O. The Human 5-HT_7 Serotonin Receptor Splice Variants: Constitutive Activity and Inverse Agonist Effects. *Br. J. Pharmacol.* **2002**, *135*, 1563−1571.
(18) Ehlen, J. C.; Grossman, G. H.; Glass, J. D. In Vivo Resetting of the Hamster Circadian Clock by 5-HT_7 Receptors in the Suprachiasmatic Nucleus. *J. Neurosci.* **2001**, *21*, 5351−5357.
(19) Smith, B. N.; Sollars, P. J.; Dudek, E. E.; Pickard, G. E. Serotonergic Modulation of Retinal Input to the Mouse Suprachiasmatic Nucleus Mediated by 5-HT_{1B} and 5-HT_7 Receptors. *J. Biol. Rhythms* **2001**, *16*, 25−38.
(20) Neumaier, J. F.; Sexton, T. J.; Yracheta, J.; Diaz, A. M.; Brownfield, M. Localization of 5-HT_7 Receptor in Rat Brain by Inmunocytochemistry, in situ Hybridization, and Agonist Stimulated cFos Expression. *J. Chem. Neuroanat.* **2001**, *21*, 63−73.
(21) Roth, B. L.; Meltzer, H. Y.; Khan,N. Binding of Typical and Atypical Antipsychotic Drugs to Multiple Neurotransmitter Receptors. *Adv. Pharmacol. (San Diego)* **1998**, *42*, 482−485.
(22) Mullins, U. L.; Gianutsos, G.; Eison, A. S. Effects of Antidepressants on 5-HT_7 Receptor Regulation in the Rat Hypothalamus. *Neuropsychopharmacology* **1999**, *21*, 352−367.
(23) Errico, M.; Crozier, R. A.; Plummer, M. R.; Cowen, D. S. 5-HT_7 Receptors Activate the Mitogen Activated Protein Kinase Extracellular Signal Related Kinase in Cultured Rat Hippocampal Neurons. *Neuroscience* **2001**, *102*, 361−367.
(24) Gill, C. H.; Soffin, E. M.; Hagan, J. J.; Davies, C. H. 5-HT_7 Receptors Modulate Synchronized Network Activity in Rat Hippocampus. *Neuropharmacology* **2002**, *42*, 82−92.
(25) Leung, E.; Walsh, L. K. M.; Pulido-Rios, M. T.; Eglen, R. M. Characterization of Putative 5-ht$_7$ Receptors Mediating Direct Relaxation in *Cynomolgus* Monkey Isolated Jugular Vein. *Br. J. Pharmacol.* **1996**, *117*, 926−930.
(26) Morecroft, I.; MacLean, M. R. 5-Hydroxytryptamine Receptors Mediating Vasoconstriction and Vasodilation in Perinatal and Adult Rabbit Small Pulmonary Arteries. *Br. J. Pharmacol.* **1998**, *125*, 69−78.
(27) Terrón, J. A.; Falcón-Neri, A. Pharmacological Evidence for the 5-HT_7 Receptor Mediating Smooth Muscle Relaxation in Canine Cerebral Arteries. *Br. J. Pharmacol.* **1999**, *127*, 609−616.
(28) Prins, N. H.; Briejer, M. R.; van Bergen, P. J. E.; Akkermans, L. M. A.; Schuurkes, J. A. J. Evidence for 5-HT_7 Receptors Mediating Relaxation of Human Colonic Circular Smooth Muscle. *Br. J. Pharmacol.* **1999**, *128*, 849−852.
(29) Centurión, D.; Sánchez-López, A.; Ortiz, M. I.; De Vries, P.; Saxena, P. R.; Villalón, C. M. Mediation of 5-HT-Induced Internal Carotid Vasodilatation in GR127935 and Ritanserin-Pretreated Dogs by 5-HT_7 Receptors. *Naunyn-Schmiedeberg's Arch. Pharmacol.* **2000**, *362*, 169−176.
(30) Howarth, C. J.; Prince, R. I.; Dyker, H.; Lösel, P. M.; Seinsche, A.; Osborne, R. H. Pharmacological Characterization of 5-Hydroxytryptamine-Induced Contractile Effects in the Isolated Gut of the Lepidopteran Caterpillar Spodoptera Frugiperda. *J. Insect Physiol.* **2002**, *48*, 43−52.
(31) De Ponti, F.; Tonini, M. Irritable Bowel Syndrome. New Agents Targeting Serotonin Receptor Subtypes. *Drugs* **2001**, *61*, 317−332.
(32) Terrón, J. A. Is the 5-HT_7 Receptor Involved in the Pathogenesis and Prophylactic Treatment of Migraine? *Eur. J. Pharmacol.* **2002**, *439*, 1−11.
(33) Forbes, I. T.; Dabbs, S.; Duckworth, D. M.; Jennings, A. J.; King, F. D.; Lovell, P. J.; Brown, A. M.; Collin, L.; Hagan, J. J.; Middlemiss, D. N.; Riley, G. J.; Thomas, D. R.; Upton, N. (*R*)-3,*N*-Dimethyl-*N*-[1-methyl-3-(4-methylpiperidin-1-yl)propyl]benzenesulfonamide: The First Selective 5-HT_7 Receptor Antagonist. *J. Med. Chem.* **1998**, *41*, 655−657.
(34) Kikuchi, C.; Nagaso, H.; Hiranuma, T.; Koyama, M. Tetrahydrobenzindoles: Selective Antagonists of the 5-HT_7 Receptor. *J. Med. Chem.* **1999**, *42*, 533−535.
(35) Lovell, P. J.; Bromidge, S. M.; Dabbs, S.; Duckworth, D. M.; Forbes, I. T.; Jennings, A. J.; King, F. D.; Middlemiss, D. N.; Rahman, S. K.; Saunders: D. V.; Collin, L. L.; Hagan, J. J.; Riley, G. J.; Thomas, D. R. A Novel, Potent, and Selective 5-HT_7 Antagonist: (*R*)-3-(2-(2-(4-Methylpiperidin-1-yl)ethyl)pyrrolidine-1-sulfonyl)phenol (SB-269970). *J. Med. Chem.* **2000**, *43*, 342−345.
(36) Kikuchi, C.; Ando, T.; Watanabe, T.; Nagaso, H.; Okuno, M.; Hiranuma, T.; Koyama, M. 2a-[4-(Tetrahydropyridoindol-2-yl)-butyl]tetrahydrobenzoindole Derivatives: New Selective Antagonists of the 5-Hydroxytryptamine7 Receptor. *J. Med. Chem.* **2002**, *45*, 2197−2206.
(37) Kikuchi, C.; Suzuki, H.; Hiranuma, T.; Koyama, M. New Tetrahydrobenzoindoles as Potent and Selective 5-HT_7 Antagonists with Increased In Vitro Metabolic Stability. *Bioorg. Med. Chem. Lett.* **2003**, *13*, 61−64.
(38) López-Rodríguez, M. L.; Porras, E.; Benhamú, B.; Ramos, J. A.; Morcillo, M. J.; Lavandera, J. L. First Pharmacophoric Hyphothesis for 5-HT_7 Antagonism. *Bioorg. Med. Chem. Lett.* **2000**, *10*, 1097−1100.
(39) *CATALYST 4.5*; Molecular Simulations Inc.: San Diego, CA 92121-3752.
(40) Smellie, A.; Kahn, S. D.; Teig, S. An Analysis of Conformational Coverage 1. Validation and Estimation of Coverage. *J. Chem. Inf. Comput. Sci.* **1995**, *35*, 285−294.
(41) Smellie, A.; Kahn, S. D.; Teig, S. An Analysis of Conformational Coverage 2. Applications of Conformational Models. *J. Chem. Inf. Comput. Sci.* **1995**, *35*, 295−304.
(42) Smellie, A.; Teig, S.; Towbin, P. Poling: Promoting Conformational Coverage. *J. Comput. Chem.* **1995**, *16*, 171−187.
(43) Brooks, B. R.; Bruccoleri, R. E.; Olafson, B. D.; States, D. J.; Swaminathan, S.; Karplus, M. CHARMm: A Program for Macromolecular Energy, Minimization, and Dynamics Calculations. *J. Comput. Chem.* **1983**, *4*, 187−217.
(44) Duffy, J. C.; Dearden, J. C.; Green, D. S. V. Use of Catalyst in the Design of Novel Non-Steroidal Anti-Inflamatory Analgesic Drugs. In *QSAR and Molecular Modeling: Concepts, Computational Tools and Biological Applications*; Sanz, F.; Giraldo, J.; Manaut, J., Eds.; Prous Science Publishers: Barcelona, 1995; pp 289−291.
(45) Halova, J.; Zak, P.; Strouf, O.; Uchida, N.; Yuzuri, T.; Sakakibara, K.; Hirota, M. Multicriteria Methodology Validation Using Catalyst Software System. A Case Study on SAR of Cathecol Analogues against Malignant Melanoma. *Org. React.* **1997**, *31*, 31−43.
(46) Daveu, C.; Bureau, R.; Baglin, I.; Prunier, H.; Lancelot, J.-C.; Rault, S. Definition of a Pharmacophore for Partial Agonists of Serotonin 5-HT_3 Receptors. *J. Chem. Inf. Comput. Sci.* **1999**, *39*, 362−369.
(47) Ekins, S.; Durst, G. L.; Stratford, R. E.; Thorner, D. A.; Lewis, R.; Loncharich, R. J.; Wikel, J. H. Three-Dimensional Quantitative Structure-Permeability Relationship Analysis for a Series of Inhibitors of Rhinovirus Replication. *J. Chem. Inf. Comput. Sci.* **2001**, *41*, 1578−1586.
(48) Saladino, R.; Crestini, C.; Palamara, A. T.; Danti, M. C.; Manetti, F.; Corelli, F.; Garaci, E.; Botta, M. Synthesis, Biological Evaluation, and Pharmacophore Generation of Uracil, 4(3*H*)-Pyrimidinone, and Uridine Derivatives as Potent and Selective Inhibitors of Parainfluenza 1 (Sendai) Virus. *J. Med. Chem.* **2001**, *44*, 4554−4562.

(49) Hirashima, A.; Morimoto, M.; Kuwano, E.; Taniguchi, E.; Eto, M. Three-Dimensional Common-Feature Hypotheses for Octopamine Agonist 2-(Arylimino)imidazolidines. *Bioorg. Med. Chem.* **2002**, *10*, 117−123.
(50) Sprague, P. W.; Hoffmann, R. Catalyst Pharmacophore Models and Their Utility as Queries for Searching 3D Databases. In *Computer Assisted Lead Finding and Optimization-Current Tools for Medicinal Chemistry*; Van de Waterbeemd H., Testa, B., Folkers, G., Eds.; VHCA: Basel, 1997; pp 230−240.
(51) López-Rodríguez, M. L.; Murcia, M.; Benhamú, B.; Viso, A.; Campillo, M.; Pardo, L. Benzimidazole Derivatives. 3. 3D-QSAR/CoMFA Model and Computational Simulation for the Recognition of 5-HT_4 Receptor Antagonists. *J. Med. Chem.* **2002**, *45*, 4806−4815.
(52) Palczewski, K.; Kumasaka, T.; Hori, T.; Behnke, C. A.; Motoshima, H.; Fox, B. A.; Le Trong, I.; Teller, D. C.; Okada, T.; Stenkamp, R. E.; Yamamoto, M.; Miyano, M. Crystal Structure of Rhodopsin: A G Protein-Coupled Receptor. *Science* **2000**, *289*, 739−745.
(53) Ballesteros, J. A.; Weinstein, H. Integrated Methods for the Construction of Three-Dimensional Models and Computational Probing of Structure−Function Relations in G-Protein Coupled Receptors. *Methods Neurosci.* **1995**, *25*, 366−428.
(54) Ballesteros, J. A.; Deupi, X.; Olivella, M.; Haaksma, E. E.; Pardo, L. Serine and Threonine Residues Bend Alpha-Helices in the chi(1) = g(−) Conformation. *Biophys. J.* **2000**, *79*, 2754−2760.
(55) López-Rodríguez, M. L.; Vicente, B.; Deupi, X.; Barrondo, S.; Olivella, M.; Morcillo, M. J.; Benhamú, B.; Ballesteros, J. A.; Salles, J.; Pardo, L. Design, Synthesis and Pharmacological Evaluation of 5-Hydroxytryptamine (1a) Receptor Ligands to Explore the Three-Dimensional Structure of the Receptor. *Mol. Pharmacol.* **2002**, *62*, 15−21.
(56) Maseras, F.; Morokuma, K. IMOMM: a New Integrated ab initio + Molecular Mechanics Geometry Optimization Scheme of Equilibrium Structures and Transition States. *J. Comput. Chem.* **1995**, *16*, 1170−1179.
(57) Tsuzuki, S.; Honda, K.; Uchimaru, T.; Mikami, M.; Tanabe, K. The Magnitude of the CH/π Interaction Between Benzene and Some Model Hydrocarbons. *J. Am. Chem. Soc.* **2000**, *122*, 3746−3753.
(58) Olivella, M.; Deupi, X.; Govaerts, C.; Pardo, L. Influence of the Environment in the Conformation of Alpha-Helices Studied by Protein Database Search and Molecular Dynamics Simulations. *Biophys. J.* **2002**, *82*, 3207−3213.
(59) Cornell, W. D.; Cieplak, P.; Bayly, C. I.; Gould, I. R.; Merz, K. M., Jr.; Ferguson, D. M.; Spellmeyer, D. C.; Fox, T.; Caldwell, J. W.; Kollman, P. A. A Second Generation Force Field for the Simulation of Proteins, Nucleic Acids, and Organic Molecules. *J. Am. Chem. Soc.* **1995**, *117*, 5179−5197.
(60) Cieplak, P.; Cornell, W. D.; Bayly, C.; Kollman, P. A. Application of the Multimolecule and Multiconformational RESP Methodology Biopolymers: Charge Derivation for the DNA, RNA and Proteins. *J. Comput. Chem.* **1995**, *16*, 1357−1377.
(61) Frisch, M. J.; Trucks, G. W.; Schlegel, H. B.; Scuseria, G. E.; Robb, M. A.; Cheeseman, J. R.; Zakrzewski, V. G.; Montgomery, J. A., Jr.; Stratmann, R. E.; Burant, J. C.; Dapprich, S.; Millam, J. M.; Daniels, A. D.; Kudin, K. N.; Strain, M. C.; Farkas, O.; Tomasi, J.; Barone, V.; Cossi, M.; Cammi, R.; Mennucci, B.; Pomelli, C.; Adamo, C.; Clifford, S.; Ochterski, J.; Petersson, G. A.; Ayala, P. Y.; Cui, Q.; Morokuma, K.; Malick, D. K.; Rabuck, A. D.; Raghavachari, K.; Foresman, J. B.; Cioslowski, J.; Ortiz, J. V.; Stefanov, B. B.; Liu, G.; Liashenko, A.; Piskorz, P.; Komaromi, I.; Gomperts, R.; Martin, R. L.; Fox, D. J.; Keith, T.; Al-Laham, M. A.; Peng, C. Y.; Nanayakkara, A.; Gonzalez, C.; Challacombe, M.; Gill, P. M. W.; Johnson, B. G.; Chen, W.; Wong, M. W.; Andres, J. L.; Head-Gordon, M.; Replogle, E. S.; Pople, J. A. *Gaussian 98*; Gaussian, Inc.: Pittsburgh, PA, 1998.
(62) Case, D. A.; Pearlman, D. A.; Caldwell, J. W.; Cheatham, T. E., III; Wang, J.; Ross, W. S.; Simmerling, C. L.; Darden, T. A.; Merz, K. M.; Stanton, R. V.; Cheng, A. L.; Vicent, J. J.; Crowley, M.; Tsui, V.; Gohlke, H.; Radmer, R. J.; Duan, Y.; Pitera, J.; Masova, I.; Seibel, G. L.; Singh, U. C.; Weiner, P. K.; Kollman, P. A. AMBER7; University of California, San Francisco, 2002.
(63) Linnanen, T.; Brisander, M.; Unelius, L.; Rosqvist, S.; Nordvall, G.; Hacksell, U.; Johansson, A. M. Atropisomeric Derivatives of 2′,6′-Disubstituted (*R*)-11-Phenylaporphine: Selective Serotonin 5-HT_7 Receptor Antagonists. *J. Med. Chem.* **2001**, *44*, 1337−1340.
(64) To, Z. P.; Bonhaus, D. W.; Eglen, R. M.; Jakeman, L. B. Characterization and Distribution of Putative 5-ht_7 Receptors in Guinea-Pig Brain. *Br. J. Pharmacol.* **1995**, *115*, 107−116.
(65) Jasper, J. R.; Kosaka, A.; To, Z. P.; Chang, D. J.; Eglen, R. M. Cloning, Expression and Pharmacology of a Truncated Splice Variant of the Human 5-HT_7 Receptor (h5-$HT_{7(b)}$). *Br. J. Pharmacol.* **1997**, *122*, 126−132.
(66) Greene, J.; Kahn, S.; Savoj, H.; Sprague, S.; Teig, S. Chemical Function Queries for 3D Database Search. *J. Chem. Inf. Comput. Sci.* **1994**, *34*, 1297−1308.
(67) Kogan, H. A.; Marsden, C. A.; Fone, K. C. F. DR4004, a Putative 5-HT_7 Receptor Antagonist, Also Has Functional Activity at the Dopamine D2 Receptor. *Eur. J. Pharmacol.* **2002**, *449*, 105−111.
(68) Aguirre, N.; Ballaz, S.; Lasheras, B.; del Río, J. MDMA ('Ecstasy') Enhances 5-HT_{1A} Receptor Density and 8-OH-DPAT-Induced Hypothermia: Blockade by Drugs Preventing 5-Hydroxytryptamine Depletion. *Eur. J. Pharmacol.* **1998**, *346*, 181−188.
(69) Cheng, Y. C.; Prusoff, W. H. Relationship Between the Inhibition Constant (K_i) and the Concentration of Inhibitor which Causes 50 Per Cent Inhibition (IC_{50}) of an Enzymatic Reaction. *Biochem. Pharmacol.* **1973**, *22*, 3099−3108.
(70) Hagan, J. J.; Price, G. W.; Jeffrey, P.; Deeks, N. J.; Stean, T.; Piper, D.; Smith, M. I.; Upton, N.; Medhurst, A. D.; Middlemiss, D. N.; Riley, G. J.; Lovell, P. J.; Bromidge, S. M.; Thomas, D. R. Characterization of SB-269970-A, a Selective 5-HT(7) Receptor Antagonist. *Br. J. Pharmacol.* **2000**, *130(3)*, 539−548.
(71) Strader, C. D.; Candelore, M. R.; Hill, W. S.; Sigal, I. S.; Dixon, R. A. F. Identification of Two Serine Residues Involved in Agonist Activation of the α-Adrenergic Receptor. *J. Biol. Chem.* **1989**, *264*, 13572−13578.
(72) Liapakis, G.; Ballesteros, J. A.; Papachristou, S.; Chan, W. C.; Chen, X.; Javitch, J. A. The Forgotten Serine. A Critical Role For Ser-$203^{5.42}$ in Ligand Binding to and Activation of the Beta 2-Adrenergic Receptor. *J. Biol. Chem.* **2000**, *275*, 37779−37788.
(73) Strader, C. D.; Fong, T. M.; Tota, M. R.; Underwood, D.; Dixon, R. A. F. Structure and Function of G Protein-Coupled Receptors. *Annu. Rev. Biochem.* **1994**, *63*, 101−132.
(74) Choudhary, M. S.; Craigo, S.; Roth, B. L. A Single Point Mutation (Phe^{340}/ Leu^{340}) of a Conserved Phenylalanine Abolishes 4-[^{125}I]-Iodo-(2,5-dimethoxy)phenylisopropylamine and [^{3}H]Mesulergine but Not [^{3}H]Ketanserin Binding to 5-Hydroxytryptamine$_2$ Receptors. *Mol. Pharmacol.* **1993**, *43*, 755−761.
(75) Steiner, T.; Koellner, G. Hydrogen Bonds with π-Acceptors in Proteins: Frequencies and Role in Stabilizing Local 3D Structures. *J. Mol. Biol.* **2001**, *305*, 535−557.
(76) Kraulis, P. J. MOLSCRIPT: A Program to Produce both Detailed and Schematic Plots of Protein Structures. *J. Appl. Crystallogr.* **1991**, *24*, 945−950.
(77) Merritt, E. A.; Bacon, D. J. Raster3D: Photorealistic Molecular Graphics. *Methods Enzymol.* **1997**, *277*, 505−524.
(78) López-Rodríguez, M. L.; Morcillo, M. J.; Fernández, E.; Porras, E.; Orensanz, L.; Beneytez, M. E.; Manzanares, J.; Fuentes, J. A. Synthesis and Structure−Activity Relationships of a New Model of Arylpiperazines. 5. Study of the Physicochemical Influence of the Pharmacophore on 5-HT_{1A}/α_1-Adrenergic Receptor Affinity: Synthesis of a New Derivative with Mixed 5-HT_{1A}/D_2 Antagonist Properties. *J. Med. Chem.* **2000**, *44*, 186−197.
(79) Lakomý, J.; Silhankova, A.; Ferles, M.; Exner, O. Studies in the Pyridine Series. XXV. Dissociation Constants of some Piperidine and Piperideine Bases. *Collect. Czech. Chem. Commun.* **1968**, *33*, 1700−1708.
(80) Bright, C.; Brown, T. J.; Cox, P.; Halley, F.; Lockey, P.; McLay, I. M.; Moore, U.; Porter, B.; Williams, R. J. Identification of a Non Peptidic RANTES Antagonist. *Bioorg. Med. Chem. Lett.* **1998**, *8*, 771−774.
(81) Pelz, K.; Protiva, M. Neurotrope und Psychotrope Substanzen XIV. 3-(4-Phenylpiperidino)propylderivative. *Collect. Czech. Chem.* **1967**, *32*, 2840−2853.
(82) Fone, K. C. F.; Marsden, C. A. Serotonin 5-HT_7 Receptors Binding to Rat Hypothalamic Membranes-Reply. *J. Neurochem.* **1999**, *72*, 883−884.
(83) Lowry, O. H.; Rosebrough, N. J.; Farr, A. L.; Randall, R. J. Protein Measurement with the Folin Phenol Reagent. *J. Biol. Chem.* **1951**, *193*, 265−275.

JM030841R